



Abnormal EEG signal energy in the elderly: A wavelet analysis of event-related potentials during a stroop task

Sergio M. Sánchez-Moguel^{a,1}, Roman Baravalle^{b,1}, Sofía González-Salinas^{a,2}, Osvaldo A. Rosso^{b,c}, Thalía Fernández^a, Fernando Montani^{b,*}

^a Departamento de Neurobiología Conductual y Cognitiva, Instituto de Neurobiología, Universidad Nacional Autónoma de México, Boulevard Juriquilla 3001, Juriquilla, Querétaro 76230, Mexico

^b Instituto de Física La Plata (IFLP), CONICET-Universidad Nacional de la Plata, La Plata, Diagonal 113 entre 63y 64, La Plata 1900, Argentina

^c Instituto de Física, Universidade Federal de Alagoas (UFAL), 57072-900 Maceió, Brazil

ARTICLE INFO

Keywords:

EEG
Wavelets
Event-related potential
Elderly
Cognitive impairment
Stroop effect

ABSTRACT

Background: Previous work showed that elderly with excess in theta activity in their resting state electroencephalogram (EEG) are at higher risk of cognitive decline than those with a normal EEG. By using event-related potentials (ERP) during a counting Stroop task, our prior work showed that elderly with theta excess have a large P300 component compared with normal EEG group. This increased activity could be related to a higher EEG signal energy used during this task.

New method: By wavelet analysis applied to ERP obtained during a counting Stroop task we quantified the energy in the different frequency bands of a group of elderly with altered EEG.

Results: In theta and alpha bands, the total energy was higher in elderly subjects with theta excess, specifically in the stimulus categorization window (258–516 ms). Both groups solved the task with similar efficiency.

Comparison with existing methods: The traditional ERP analysis in elderly compares voltage among conditions and groups for a given time window, while the frequency composition is not usually examined. We complemented our previous ERP analysis using a wavelet methodology. Furthermore, we showed the advantages of wavelet analysis over Short Time Fourier Transform when exploring EEG signal during this task.

Conclusions: The higher EEG signal energy in ERP might reflect undergoing neurobiological mechanisms that allow the elderly with theta excess to cope with the cognitive task with similar behavioral results as the normal EEG group. This increased energy could promote a metabolic and cellular dysregulation causing a greater decline in cognitive function.

1. Introduction

Healthy aging is accompanied by a natural detriment of physical and cognitive abilities (Román Lapuente and Sánchez Navarro, 1998). In particular, inhibitory control (Rey-Mermet and Gade, 2018; Thomas et al., 2010) and attention (Diamond, 2020; Thomas et al., 2010) are importantly affected. Changes in brain electrical activity, which can be measured noninvasively by the EEG, are tightly related to the aforementioned cognitive processes (Buzsáki, 2006; Lopes da Silva, 2011). Some authors have proposed that changes in the EEG of the elderly, obtained under resting conditions, are not only the result of normal

aging but can contain signs of undergoing subclinical pathologic processes (Chang et al., 2011). Moreover, excess in delta and theta frequency bands of resting EEG from the healthy elderly, compared to a normative base according to age, is an excellent predictor of cognitive detriment in the following seven years (Prichep et al., 2006; van der Hiele et al., 2008). We recently showed that the healthy elderly with an excess of theta EEG activity have impairments in inhibitory control processing at the electrophysiological level (Sánchez-Moguel et al., 2018).

Stroop tasks have been used during event-related potentials (ERP) and functional magnetic resonance imaging (fMRI) to study the decrease

* Corresponding author.

E-mail address: f.montani@fisica.unlp.edu.ar (F. Montani).

¹ Both authors contributed equally to the current project

² Present address: Genetics Department. Rutgers University. Piscataway, NJ 08854, USA.

in the efficiency of inhibitory processing during healthy and pathological aging (Amieva, 2004; Kaufmann et al., 2008; Ramos-Goicoa et al., 2016; Sánchez-Moguel et al., 2018; West and Alain, 2000). An over-recruitment of neuronal activity during aging was observed using fMRI during the performance of Stroop tasks; this enhanced neuronal activity is proposed to have a compensatory function (Cabeza, 2002; Cabeza et al., 2004; Langenecker et al., 2004; Mathis et al., 2009; Milham et al., 2002; Zysset et al., 2007). Furthermore, fMRI studies showed a higher brain activity in older people with mild cognitive impairment (MCI) compared to the healthy elderly (Kaufmann et al., 2008).

In our earlier work, we showed that the elderly with theta excess have a larger P300 component associated with stimulus categorization than the elderly with a normal EEG (Sánchez-Moguel et al., 2018). A higher voltage in ERP is related to higher synchronized neuronal activity that would be associated with a greater amount of energy. However, the changes in EEG signal energy associated with any cognitive process in the elderly with excess in theta activity have not been yet properly quantified. As the elderly with excess in theta activity are probably in a previous stage of MCI, we hypothesize that they might already be having a dysregulation in EEG signal energy during the performance of an inhibitory control task (Mattson and Arumugam, 2018).

Wavelet transform (WT) can help us to compare the EEG signal energy across bands during the performance of Stroop tasks. The main advantage of wavelet analysis over Fourier analysis is the flexible (and optimal) time-frequency resolution (Daubechies, 1992; Mallat, 2008). Thus, we can follow the brain frequency dynamics over time (Daubechies, 1992; Mallat, 2008; Rosso et al., 2006). The wavelet analysis allows us to have a standard frequency decomposition of EEG signals over time (Daubechies, 1992; Goupillaud et al., 1984; Mallat, 2008; Rosso et al., 2006, 2005). This is a desirable property, because we can track the frequency variations of the EEG signal over time and detect at which time window of the Stroop task changes in signal energy occur.

The general objective of this study was to explore, using WT, whether there were differences in EEG signal energy across frequency bands in ERP during the performance of a counting Stroop task between a group of elderly subjects with an excess of theta activity in their resting state EEG and another one with normal EEG. The specific objective was to evaluate the EEG signal energy between groups for each of the frequency bands (i.e., delta, theta, alpha, beta, and gamma) across different time windows of the ERP. We expected to provide a precise quantification of EEG signal changes in the group with theta excess, specifically in the time window associated with the stimuli categorization.

2. Materials and methods

2.1. Participants

Forty-six healthy older adults aged over 60 years were recruited to participate in the study (26 females). The inclusion criteria were to be right-handed, to have more than nine years of schooling, to have an average level of intelligence (Wechsler Intelligence Scale for adults 90–190, (Wechsler, 2003)), and not to have any psychiatric disorder according to their age (NEUROPSI, (Ostrosky-Solis et al., 1999)); Q-LES-Q questionnaire, > 70% (Endicott et al., 1993); Mini-Mental State Examination, > 27 (Reisberg et al., 2008, 1982); Global Deterioration Scale, 1–2 (Reisberg et al., 2008, 1982); Alcohol Use Disorders Identification Test, < 5 (Babor et al., 2001); Beck Depression Inventory, < 4 (Beck et al., 1961); Geriatric Depression Scale, < 5 (Yesavage et al., 1982). Furthermore, subjects had no signs of chronic diseases such as diabetes or hypercholesterolemia. The subjects were classified into two groups according to the characteristics of their EEG. Subjects in the Normal-EEG group presented normal EEGs, from both the quantitative and qualitative points of view, and subjects in the Theta-EEG group presented an excess of theta activity for their age in at least one electrode, which is further described below. Each group was formed by 23 participants. The project was approved by the bioethics committee of

the Neurobiology Institute of the National Autonomous University of Mexico (UNAM). ERP analyses of the participants were published by Sánchez-Moguel et al. (2018) and are further analyzed here using wavelets.

2.2. EEG analysis in resting condition

Based on the next analysis, participants were classified as with a normal EEG (Normal-EEG group) or with excess in the theta band (Theta-EEG group); 23 subjects made up each group (13 females in each group).

The EEG from 19 tin electrodes (10–20 International System, ElectroCap™, International Inc., Eaton, Ohio) referenced to linked earlobes was recorded from each subject in the resting condition with eyes closed using a MEDICID™ IV system (Neuronic Mexicana, S.A., Mexico) and Track Walker™ v5.0 data system for 15 min. The EEG was digitized using the MEDICID IV System (Neuronic A.C.) with a sampling rate of 200 Hz using a band-pass filter of 0.5 – 50 Hz, and the impedance was kept below 5 kΩ. Twenty-four artifact-free segments of 2.56 s each were selected, and the quantitative EEG analysis was performed offline using the fast Fourier transform to obtain the power spectrum every 0.39 Hz; also the geometric power correction (Hernández et al., 1994) was applied, and absolute (AP) and relative power (RP) in each of the four classic frequency bands were obtained: Delta (1.5–3.5 Hz), theta (3.6–7.5 Hz), alpha (7.6–12.5 Hz), and beta (12.6–19 Hz). These frequency ranges were the same as those used for the normative database (Valdés et al., 1990) provided by MEDICID IV. Z-values were obtained for AP and RP, comparing the subject's values with values of the normative database [$Z = (x - \mu) / \sigma$, where μ and σ are the mean value and the standard deviation of the normative sample of the same age as the subject, respectively]. Z-values > 1.96 in the theta band were considered abnormal ($p < 0.05$) and therefore this was the criteria for inclusion in the Theta-EEG group.

2.3. Counting stroop task

In the counting Stroop task, subjects are asked to answer how many words are presented in a slide, regardless of the meaning of the word itself (Bush et al., 2006). Subjects increase their response times and tend to make more mistakes when the meaning of the word does not match the number of times that the word appears; this phenomenon is known as the Stroop or interference effect (MacLeod, 1991).

2.3.1. Behavioral task

Series of one, two, three, or four words that denote numbers (“one”, “two”, “three”, “four”) were presented in the center of a 17-inch computer screen. Time presentation of the stimuli was 500 ms, and the interstimulus interval was 1500 ms. An incongruent condition, herein referred to as Interference stimulus, consisted of a trial where the number of presented words did not correspond with the meaning of the word. The congruent condition, further referred to as No Interference stimulus, consisted of a trial in which the number of presented words and the meaning of the word that was presented matched. A total of 120 Interference and 120 No Interference stimuli were randomly presented.

Subjects were asked to indicate the number of times that the word appeared in each trial, using a response pad held in their hands. One-half of the participants used their left thumbs to answer “one” or “two” and their right thumbs to indicate “three” or “four”; the other half of the participants used their opposite hand to counterbalance the motor responses. The participants were asked to answer as quickly and accurately as possible. We ensured that the participants understood the instructions by presenting a brief practice task before the experimental session.

2.4. ERP acquisition and analysis

The EEGs were recorded with 32 Ag/AgCl electrodes mounted on an elastic cap (Electrocap) while the participant performed the counting Stroop task, using NeuroScan SynAmps amplifiers (Compumedics NeuroScan) and the Scan 4.5 software (Compumedics NeuroScan). Electrodes were referenced to the right earlobe (A2), and the electrical signal was collected from the left earlobe (A1) as an independent channel. Recordings were re-referenced offline in two ways: (a) to the averaged earlobes, as was usually performed in previous studies, and (b) to the average reference. The EEG was digitized with a sampling rate of 500 Hz using a band-pass filter of 0.01–100 Hz. Impedances were kept below 5 k Ω . An electrooculogram was recorded using a supraorbital electrode and an electrode placed on the outer canthus of the left eye.

ERPs were obtained for each subject and experimental condition (i. e., No Interference and Interference). Epochs of 1500 ms were obtained for each trial, which consisted of 200 ms pre-stimulus and 1300 ms post-stimulus intervals. An eye movement correction algorithm (Gratton et al., 1983) was applied to remove blinks and vertical ocular-movement artifacts. Low-pass filtering for 50 Hz and a 6-dB slope was performed offline. A baseline correction was performed using the 200 ms pre-stimulus time window, and a linear detrend correction was performed on the whole epoch. Epochs with voltage changes exceeding $\pm 80 \mu\text{V}$ were automatically rejected from the final average. The epochs were visually inspected, and those with artifacts were also rejected. Averaged waveforms for each subject and each stimulus type included only those trials that corresponded to correct responses. Only the correct answers were used for further analysis because we had a low percentage of incorrect answers, which made the ERP analysis for incorrect answers unreliable.

2.5. Wavelet transform and wavelet-based measures

The ERPs were next subjected to a wavelet analysis. Unlike Fourier analysis, in which the sine and cosine functions are used, the wavelet transform is based on functions that are vanishing oscillating functions (Mallat, 2008; Rosso et al., 2006). A wavelet is an oscillating function with an amplitude that begins at zero, increases, and then decreases to zero. In other words, it is an oscillating function with compact support. One of the interesting properties of these functions is that they are well localized in time and in frequency, so they are functions which cover a certain narrow frequency band (Daubechies, 1992; Mallat, 2008). Defining one function $\psi(t)$ as being the first scale of the analysis, we can continue decomposing the signal into subsequent scales, by scaling and translating this function. This $\psi(t)$ function, an oscillating function with narrow width both in time and space, is called the mother wavelet. Using a scale and translation parameters $a, b \in \mathbb{R}$, $a \neq 0$, we can construct a filter bank to decompose the signal into frequency bands (Daubechies, 1992; Mallat, 2008). In the continuous wavelet transform these parameters are arbitrary, whereas in the case of the fast discrete wavelet transform an algorithm exists which selects the scale and translation parameters by means of a dyadic decomposition, which would be detailed later in this section (Mallat, 2008). Within the wavelet multi-resolution decomposition framework, a wavelet family $\psi_{a,b}$ is a set of elemental functions generated by scaling and translating a unique admissible mother wavelet $\psi(t)$:

$$\psi_{a,b} = |a|^{-\frac{1}{2}} \psi\left(\frac{t-b}{a}\right) \quad (1)$$

where $a, b \in \mathbb{R}$, $a \neq 0$ are the scale and translation parameter, respectively, and t is the time (Rosso et al., 2006). In defining the mother wavelet, one chooses the wavelet functions from a subspace of the space $L^1(\mathbb{R}) \cap L^2(\mathbb{R})$. This is the space of functions with finite integral of its absolute value and finite integral of its squared absolute value. This ensures that the wavelet could have zero mean and could be normalized

as $\|\psi(t)\|^2 = 1$. In the context of signal analysis this means that the wavelet has zero mean and energy equal to 1. In most situations it is useful to restrict the mother wavelet to be a continuous function with a higher number N of vanishing moments, i.e. for all integer $m < N$, $\int_{-\infty}^{\infty} t^m \psi(t) dt = 0$. This is the case of the Daubechies- N wavelets, with N the number of vanishing moments (Daubechies, 1992).

Wavelet's transformation has been widely used in EEG signal processing (Al Ghayab et al., 2019; Blanco et al., 1995, 1996, 1997, 1998; Gross, 2014; Korol et al., 2007; Kovach and Gander, 2016; Lopes-Dos-Santos et al., 2018; Nakhnikian et al., 2016; Navajas et al., 2013; Quian Quiroga et al., 1997; Quiroga et al., 2001; Rosenblatt et al., 2014; Rosso et al., 2001; Rosso et al., 2004; Rosso and Hyslop et al., 2005; Rosso et al., 2005; Schrouff et al., 2016; Schütt et al., 2003; Venkata Phanikrishna and Chinara, 2021; Yordanova et al., 2002; Rosso et al., 2006). It divides the continuous signal into time frequency domains. Provides high frequency resolution for low frequency content and high time resolution for its high frequency coverage. Wavelet transform is considered an effective tool for analysis of non-stationary signals such as brain wave signals (Lopes-dos-Santos et al., 2015; Quian Quiroga and Panzeri, 2009; Quian Quiroga et al., 2001; Ortiz-Rosario et al., 2015; Rosso et al., 2001; Rosso et al., 2004; Rosso and Hyslop et al., 2005; Rosso et al., 2005; Schrouff et al., 2016; Schütt et al., 2003; Venkata Phanikrishna and Chinara, 2021; Yordanova et al., 2002). The wavelet coefficients examine the correlations across the signal under investigation and the set of functions named as wavelets. These wavelets are acquired among the translation and dilatation of some special functions named as mother wavelets and the coefficients show the correspondence between the investigated signal and the wavelets (Al Ghayab et al., 2019; Blanco et al., 1995, 1996, 1997, 1998; Gross, 2014; Korol et al., 2007; Kovach and Gander, 2016; Lopes-Dos-Santos et al., 2018; Nakhnikian et al., 2016; Navajas et al., 2013; Quian Quiroga et al., 1997, 2001; Rosenblatt et al., 2014; Rosso et al., 2001, 2004, 2005; Rosso and Hyslop et al., 2005; Schrouff et al., 2016; Schütt et al., 2003; Venkata Phanikrishna and Chinara, 2021; Yordanova et al., 2002).

The wavelet treatment of brain EEG signals has been presented previously by some of the authors of this paper (Baravalle et al., 2018; Blanco et al., 1995; Blanco et al., 1996; Blanco et al., 1997; Blanco et al., 1998; Korol et al., 2007; Quian Quiroga et al., 1997; Quian Quiroga et al., 2001; Rosso et al., 2001; Rosso et al., 2004; Rosso and Hyslop et al., 2005; Rosso et al., 2005; Rosso et al., 2005; Schütt et al., 2003; Yordanova et al., 2002; Rosso et al., 2006). It can be considered today as the state-of-the-art in these matters that there are multiple possible choices for the specific type of wavelet and that the election of the type of wavelet does not affect the results (Baravalle et al., 2018; Blanco et al., 1995; Blanco et al., 1996; Blanco et al., 1997; Blanco et al., 1998; Korol et al., 2007; Quian Quiroga et al., 1997; Quian Quiroga et al., 2001; Rosso et al., 2001; Rosso et al., 2004; Rosso and Hyslop et al., 2005; Rosso et al., 2005; Schütt et al., 2003; Yordanova et al., 2002; Rosso et al., 2006). This is to say the adopted methodology is robust and independent of the type of wavelet that could be adopted for the analysis (Baravalle et al., 2018; Blanco et al., 1995; Blanco et al., 1996; Blanco et al., 1997; Blanco et al., 1998; Korol et al., 2007; Quian Quiroga et al., 1997; Quiroga et al., 2001; Rosso et al., 2001; Rosso et al., 2004; Rosso and Hyslop et al., 2005; Rosso et al., 2005; Schütt et al., 2003; Yordanova et al., 2002; Rosso et al., 2006). For the sake of completeness we show a detailed comparison of the different mother wavelet methodologies in the Appendix A, Figs A1, A2, A3, A4 and A5.

Let us remark that by choosing the wavelet function, we need to look at the resolution of the wavelet in both time and frequency domains. Due to the uncertainty principle, a shorter-in-time wavelet is going to be wider in frequency space, and vice versa. But this property, critical in using wavelets as a filter bank to reconstruct or compress the signal, is not so important when studying the power spectra (Torrence and

Compo, 1998). In this paper we use the Daubechies 2 as a mother wavelet, which means that this wavelet has zero mean and zero variance (Baravalle et al., 2018). We tested with other wavelets, from the family of Daubechies, Symlets and Fejér-Korovkin (Nielsen, 2001), but the quantitatively and qualitatively results were very similar. The only variant of the different approaches, being in all cases which mother wavelet can be used, is an orthogonal discrete mother wavelet and therefore its election may depend on what is the choice made by the author. In all of them, the specific methodology is basically the same. There are multiple possible choices for the specific type of wavelet, however, the election of the type of wavelet does not affect the results. Notice that we presented a detailed description of the wavelet methodology and we could also exhibit all different possible mother wavelets that are being used in the literature, however, we consider this to be slightly redundant for the objective of this article as the election of the type of wavelet does not affect the results (Baravalle et al., 2018; Blanco et al., 1995; Blanco et al., 1996; Blanco et al., 1997; Blanco et al., 1998; Korol et al., 2007; Quian Quiroga et al., 1997; Quiroga et al., 2001; Rosso et al., 2001; Rosso et al., 2004; Rosso and Hyslop et al., 2005; Rosso et al., 2005; Schütt et al., 2003; Yordanova et al., 2002; Rosso et al., 2006). Importantly, in other papers published also by the authors of this paper, we have included the treatment with Gabor Transform, with variant of time-frequency analysis, and a comparison with other mother wavelets finding no differences (Baravalle et al., 2018; Blanco et al., 1995; Blanco et al., 1996; Blanco et al., 1997; Blanco et al., 1998; Korol et al., 2007; Quian Quiroga et al., 1997; Quiroga et al., 2001; Rosso et al., 2001; Rosso et al., 2004; Rosso and Hyslop et al., 2005; Rosso et al., 2005; Schütt et al., 2003; Yordanova et al., 2002; Rosso et al., 2006).

The continuous wavelet transform (CWT) of a signal $S(t) \in L^2(\mathbb{R})$ (the space of real square summable functions) is defined as the correlation between the signal $S(t)$ and the wavelet family $\psi_{a,b}$ for each a and b :

$$\langle S, \psi_{a,b} \rangle = |a|^{\frac{1}{2}} \int_{-\infty}^{\infty} S(t) \psi^* \left(\frac{t-b}{a} \right) dt, \quad (2)$$

where $*$ means complex conjugation. In principle, the CWT gives a highly redundant representation of the signal because it produces an infinite number of coefficients (Rosso et al., 2006). A nonredundant and efficient representation is given by the discrete wavelet transform (DWT), which also ensures complete signal reconstruction. One way to fulfill this condition is by means of the fast wavelet transform algorithm (Mallat, 2008). In this case, for a special selection of the mother wavelet function $\psi(t)$ and the discrete set of parameters $a_j = 2^j$ and $b_{j,k} = 2^j k$, with $j, k \in \mathbb{Z}$, the family $\psi_{j,k}(t) = 2^{j/2} \psi(2^j t - k)$ constitutes an orthonormal basis of $L^2(\mathbb{R})$ (Mallat, 2008). This orthonormality is the basis of the multiresolution analysis, and ensures that each subspace spanned by a set of functions with an integer index j is independent of the subspace spanned by functions with an integer index $j' \neq j$. Any arbitrary function of this space can therefore be uniquely decomposed, and the decomposition can be inverted (Daubechies, 1992; Mallat, 2008; Rosso et al.,

2006). The wavelet coefficients of the DWT are $\langle S, \psi_{j,k} \rangle = C_j(k) =$

$$|2|^{-\frac{j}{2}} \int_{-\infty}^{\infty} S(t) \psi^* \left(\frac{t-2^{-j}k}{2^{-j}} \right) dt \text{ (Mallat, 2008). The DWT produces only}$$

as many coefficients as there are samples within the signal under analysis $S(t)$, without any loss of information.

Due to the Nyquist theorem, frequencies above half the sampling frequency cannot be distinguished (Nyquist, 1928; Shannon, 1949). The intuition behind the DWT is that for each scale the signal is separated using a lowpass filter (this part is called the signal approximation at that scale) and a highpass filter (this part is called the detail signal). This decomposition is done into octave bands, i.e. at each scale j the

frequency range of the signal approximation is divided into two parts: the approximation and the detail signals at scale $j+1$ (Daubechies, 1992; Mallat, 2008). The subbands (in Hz) for the signal approximation at level j are approximately $\left[n \frac{F_s}{2^{j+1}}, (n+1) \frac{F_s}{2^{j+1}} \right)$, with $n = 0, \dots, 2^j - 1$ and F_s the sampling frequency. Let us assume that the signal is given by equally sampled values $S = \{s_0(n), n = 1, \dots, M\}$, with M being the total number of samples. If the decomposition is carried out over all possible scales (or resolution levels), $N = \log(M)$, the wavelet expansion reads:

$$S(t) = \sum_{j=-N}^{-1} \sum_k C_j(k) \psi_{j,k}(t) = \sum_{j=-N}^{-1} r_j(t), \quad (3)$$

where the wavelet coefficients $C_j(k)$ can be interpreted as the local residual errors between successive signal approximations at scales j and $j-1$, respectively, and $r_j(t)$ is the detail signal at scale j , which contains information of the signal $S(t)$ corresponding to the frequencies $2^{j-1} F_s \leq |F| < 2^j F_s$, F_s being the sampling frequency (Rosso et al., 2006, 2005). For example, the first step in the DWT is the following: at scale $j=0$ we have the original signal $S(t)$. We decompose at level $j=1$ the signal into the approximation (lowpass) and detail (highpass) signals $A1$ and $D1$, respectively. Thus, $S(t) = A1(t) + D1(t)$. Here $A1$ and $D1$ are functions of orthonormal spaces, thus they are linearly independent. In this case, we have that $D1(t) = S(t) - A1(t)$. For the scale $j=2$, we take $A1$ and decompose it in approximation and detail signals for scale $j=2$, $AA2$ and $AD2$, respectively. Since the DWT algorithm is done in a recursive way, at scale j we have the decomposition in lowpass (signal approximation at scale j) and highpass frequencies (detail signal at scale j) of the signal approximation at scale $j-1$. The highpass filtering is done using the wavelet function for this scale, $\psi_{j,k}(t)$, so the wavelet coefficients give the highpass content of the signal approximation in the previous scale $j-1$. Thus, if we subtract the signal approximation at scales $j-1$ and j , we recover the detail signal at scale j , which is given by the wavelet coefficients. That is the reason why these wavelet coefficients can be interpreted as the local residual error between successive signal approximations (Mallat, 2008).

Since the family $\psi_{j,k}(t)$ is an orthonormal basis for $L^2(\mathbb{R})$, the concept of wavelet energy is similar to the Fourier theory energy. Thus the signal energy at each resolution level, $j = -1, \dots, -N$, will be the energy of the detail signal:

$$E_j = \|r_j\|^2 = \sum_k |C_j(k)|^2. \quad (4)$$

The units of energy here are the same as in Fourier spectra, i.e. the units of the squared amplitude of the signal (μV^2 in this case). Since the signal energy of the wavelet function is 1, the DWT conserves the signal energy. The total energy can be obtained summing over all the resolution levels

$$E_{total} = \|S\|^2 = \sum_{j=-N}^{-1} \sum_k |C_j(k)|^2 = \sum_j E_j \quad (5)$$

Finally, we define the relative wavelet energy (RWE) through the normalized ρ_j values:

$$\rho_j = \frac{E_j}{E_{total}} \quad (6)$$

for the resolution levels $j = -1, -2, \dots, -N$. The distribution $P \equiv \{\rho_j\}$ can be viewed as a time-scale distribution, which is a suitable tool for detecting and characterizing phenomena in the time and frequency domains (Rosso et al., 2006). Since the mother wavelet has a certain width in frequency domain, in wavelet theory the term scale is used instead of the term frequency. Moreover, in the DWT the partition of the frequency range is done in a dyadic way (Mallat, 2008). That is, for each scale, the lower frequency signal (signal approximation) is filtered into two frequency ranges, whereas the high frequency signal (signal detail)

Table 1

Frequency for each band analyzed. Intervals for each band when analyzing five windows with wavelets.

| Band | Frequency Interval (Hz) |
|-------|-------------------------|
| Delta | [1.9531 – 3.9063] |
| Theta | [3.9063 – 7.8125] |
| Alpha | [7.8125 – 11.7188] |
| Beta | [11.7188 – 19.5313] |
| Gamma | [19.5313 – 39.0625] |

Table 2

Frequency for each band when comparing wavelet and STFT methodologies. Intervals for each band when analyzing ten windows.

| Band | Frequency Interval (Hz) | |
|-------------|-------------------------|-------------------|
| | Wavelets | STFT |
| Delta+Theta | [0, 7.8125] | [0, 7.6923] |
| Alpha+Beta | [7.6923, 15.3846] | [7.8125, 15.625] |
| Gamma | [15.3846, 38.4615] | [15.625, 39.0625] |

Table 3

Behavioral performance during the counting Stroop task. Data are shown as mean \pm standard deviation (SD); response times are expressed in ms.

| Group | Stimulus | % Correct responses | Response times |
|------------|-----------------|---------------------|--------------------|
| Normal-EEG | Interference | 77.13 \pm 14.93 | 727.47 \pm 59.21 |
| | No Interference | 83.55 \pm 14.28 | 658.97 \pm 59.13 |
| Theta-EEG | Interference | 74.63 \pm 19.55 | 698.71 \pm 72.81 |
| | No Interference | 83.15 \pm 17.14 | 656.10 \pm 70.93 |

remains unchanged. Thus, the resolution in frequency changes for lower or higher frequencies, in contrast with the windowed Short Time Fourier Transform, in which the resolution in time and frequency is the same for all the frequencies. However, within the DWT one can localize with certain precision the frequency bands for each scale, as $\left(\left[n \frac{F_s}{2^{j+1}}, (n+1) \frac{F_s}{2^{j+1}} \right) \right)$, with $n = 0, \dots, 2^j - 1$ and F_s the sampling frequency. The quality of this bandpass approximation depends on how frequency-localized the mother wavelet is. We tested the results with a very localized wavelet, the Fejér-Korovkin 18, and the result was the same as with the Daubechies 2 we used (Nielsen, 2001).

An extension of this discrete wavelet transform is the discrete wavelet packet transform (DWPT). The DWPT is a generalization of the DWT that at level j of the transform partitions the frequency axis into 2^j equal width frequency bands $\left(\left[n \frac{F_s}{2^{j+1}}, (n+1) \frac{F_s}{2^{j+1}} \right) \right)$, with $n = 0, \dots, 2^j - 1$, and F_s the sampling frequency. Increasing the transform level increases frequency resolution, but starting with a series of length M , at level j there are only $M/2^j$ DWPT coefficients for each frequency band n (Percival and Walden, 2000). That is, the DWPT could be used as a non-redundant description of the signal. Thus, the DWPT is the same as the DWT for the signal approximation, but it also filters at each scale the detail (high frequency) signal. In this case, one can have a good frequency resolution also for higher frequencies (Coifman and Wickhauser, 1992; Mallat, 2008).

The wavelet packets can be organized on an orthonormal basis of the space of finite energy signals. The main advantage of using wavelet packets is that the standard wavelet analysis can be extended with a flexible strategy. Thus the description of the given signal can be well adapted according to the significant structures (Blanco et al., 1998). The resulting DWPT yields what can be called a time-scale-frequency decomposition because each DWPT coefficient can be localized to a particular band of frequencies and a particular interval of time (Percival and Walden, 2000). Here we use the flexibility of the DWPT to combine the energy of the decomposition frequency bands, to have an insight into the typical clinical frequency band decomposition: delta, theta, alpha,

beta, and gamma. Finally, we have the energy $\{E_{Delta}, E_{Theta}, E_{Alpha}, E_{Beta}, E_{Gamma}\}$ corresponding to each band, and the relative energy $\{\rho_{Delta}, \rho_{Theta}, \rho_{Alpha}, \rho_{Beta}, \rho_{Gamma}\}$ for each one of the five bands. The energy corresponding to each band is obtained by adding all the values of E_j for all the j values that satisfy $2^{j-1}F_s \leq |F| \leq 2^jF_s$, F_s being the sampling frequency and $|F|$ being within the frequency interval corresponding to one of the five clinical frequencies. We used the frequency band intervals shown in Table 1 for the results presented in Sections 3.2, 3.3, 3.4, and 3.5.

Regarding time-frequency analysis, one of the first developed methodologies is the Short Time Fourier Transform (STFT). STFT is a well-known technique in signal processing to analyze non-stationary signals. STFT segments the signal into narrow time intervals and takes the Fourier transform of each segment (Allen, 1977). This allows us to obtain the frequency spectra for each time-window. However, one of the pitfalls of the STFT is that it has a fixed resolution. The problem with this fixed resolution comes from example when studying a signal in which a combination of high-frequency and low-frequency events occur. For the STFT to distinguish the frequency of low-frequency events a larger time window is needed, but this is detrimental to the temporal resolution of the high-frequency events (Daubechies, 1992). This is one of the motivations for using wavelet transform and multiresolution analysis, which can give good time resolution for high-frequency events and good frequency resolution for low-frequency events (Daubechies, 1992; Mallat, 2008). As an example of this resolution issue with the STFT, we can look at Table 2. When segmenting the signal into ten time windows, frequency resolution is lost with STFT, at the point that two bands need to be merged: delta+theta and alpha+beta, whereas with wavelets these bands can yet be distinguished, as in Table 1 (with the exception that with ten time windows the delta band includes the range [0 – 3.9063] Hz as discussed in Section 3.6). The comparison of wavelets and STFT using the frequency band intervals shown in Table 2 was performed in Section 3.6.

2.6. Statistical analysis

The behavioral data from the counting Stroop task, and the total and relative energy were tested for Normal distribution using the Shapiro-Wilk test, Lilliefors test, and Qqplots. Most of the data followed a Normal distribution and to facilitate the description of the data we used ANOVAs. The data were also analyzed using nonparametric tests reaching to the same conclusions as with ANOVAs; these results are available upon request. ANOVAs included repeated measures for Stimulus, Bands, and Windows, as required. A Tukey post hoc test was used to make comparisons among groups. Data were processed, analyzed, and plotted using R and Matlab.

3. Results

The participants were examined for their general health status and those that meet the criteria described in Materials and Methods were then assessed as described next. After the participants were categorized into Normal-EEG or Theta-EEG by resting state analysis of their EEG they were tested in the counting Stroop task while their EEG was also recorded. Data were processed following standard procedures for ERP analysis (Sánchez-Moguel et al., 2018) and were later examined by wavelet analysis.

3.1. Behavioral results of the counting stroop task

We first explored if there were behavioral differences during the execution of the task. Table 3 shows the mean percentage of correct responses and response times (RT) by each group and type of stimulus. For the RT, there was no main effect of Group ($F(1, 44) = 0.73$, $p = 0.3963$), while Stimulus and the Group X Stimulus interaction were significant (Stimulus: $F(1, 44) = 85.89$, $p < 0.0001$; Group X Stimulus: F

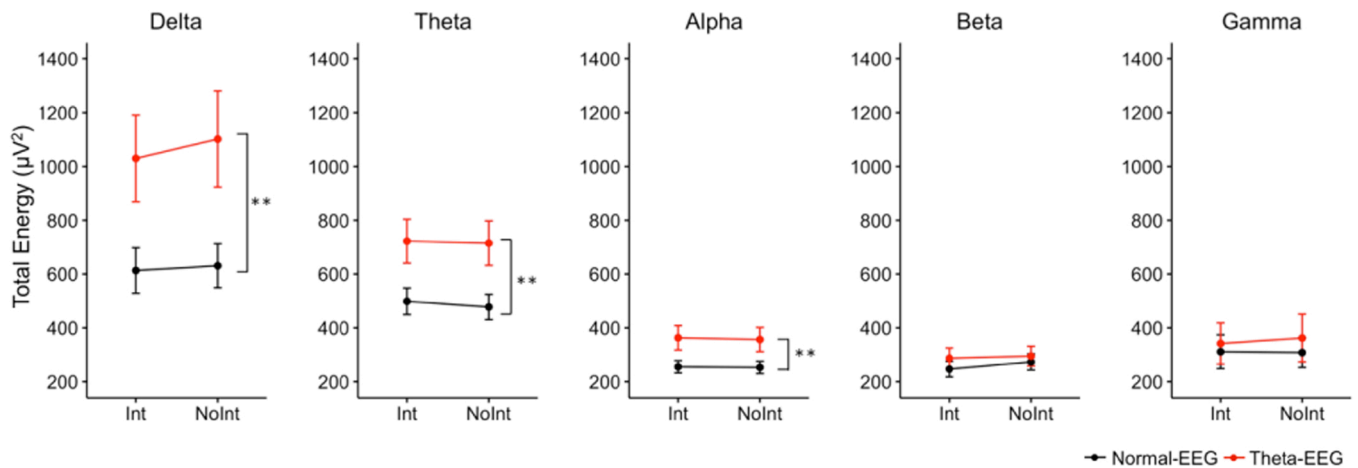


Fig. 1. Total energy. Data were obtained from the average total energy across electrodes (reference electrodes excluded) for Interference (Int) and No Interference (NoInt) stimuli during the counting Stroop task. ** $p < 0.01$ for group factor from two-way ANOVA. Data are expressed as means with standard error bars.

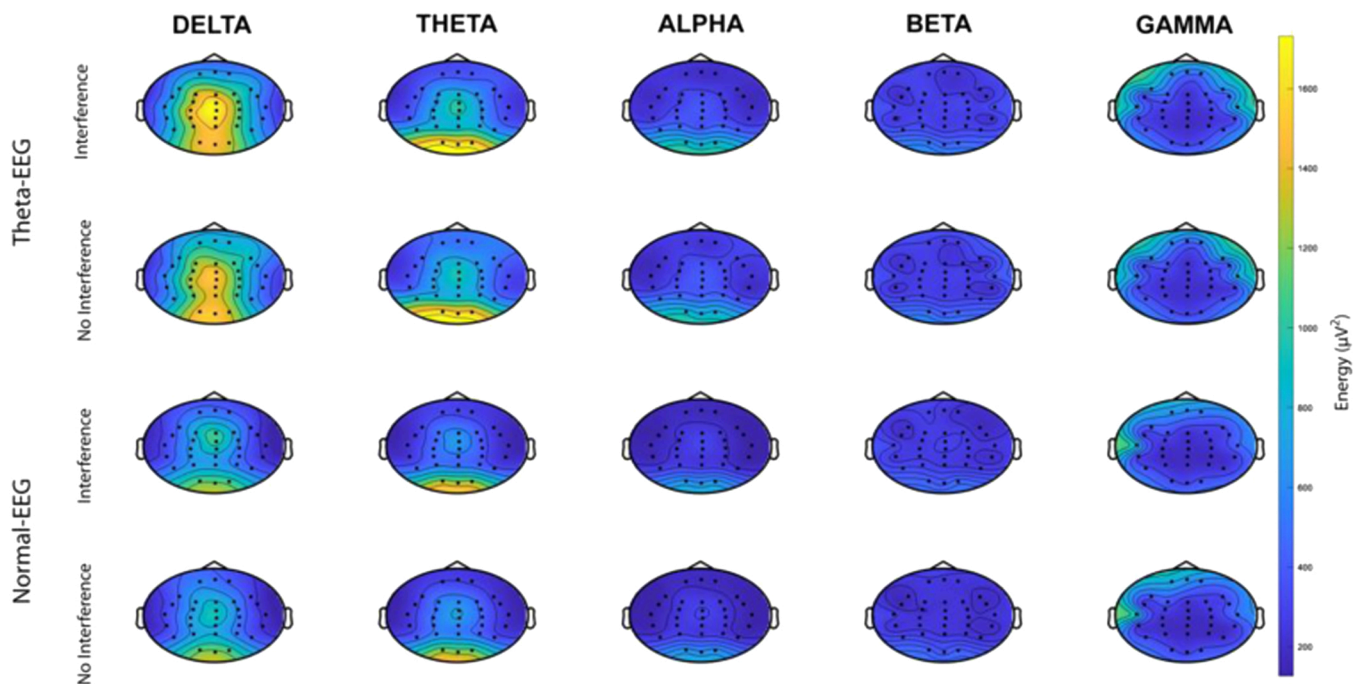


Fig. 2. Topographic distribution of total energy. Total energy is shown for the different bands during Interference and No Interference stimuli according to the EEG group. The color scale is expressed in μV^2 . (For interpretation of the references to colour in this figure, the reader is referred to the web version of this article.)

(1, 44) = 4.66, $p = 0.0363$). Post hoc analysis showed that RT for the Interference stimuli were larger than the response times for No Interference stimuli within both the Theta-EEG (mean difference (MD) = 42.61 ms, $p < 0.001$) and the Normal-EEG groups (MD = 68.5 ms, $p < 0.001$); the Theta-EEG group showed fewer differences between stimulus types than the Normal-EEG group. There were no differences between groups for the same type of stimulus (Interference: $p = 0.39$, No Interference $p = 0.99$). We applied the arcsine to the percentage of correct responses in order to approximate the distribution of the data to a Gaussian distribution to use parametric statistical tests. We observed a significant main effect of Stimulus ($F(1, 44) = 62.43$, $p < 0.0001$) with a lower percentage of correct answers in the Interference than in the No Interference condition; however, there were no main effects of Group or Group X Stimulus interaction (Group: $F(1, 44) = 0.09$, $p = 0.76$, Group X Stimulus: $F(1, 44) = 1.24$, $p = 0.27$). These results showed that, at the behavioral level, the Theta-EEG and Normal-EEG groups showed a

Stroop effect and that they answered similarly despite the differences in their resting EEG.

3.2. Total energy

We wanted to explore whether the higher theta activity found in the Theta-EEG group under resting state conditions was still present during the performance of a task that evaluates inhibitory processing, a cognitive dimension known to be compromised during ageing (Rey-Mermet and Gade, 2018; Sánchez-Moguel et al., 2018; Thomas et al., 2010). Furthermore, we were interested in exploring whether abnormal EEG signal activity was present in other frequency bands.

We first compared the total energy on each band between Theta-EEG and Normal-EEG groups, obtaining the average of the total energy for all electrodes (reference electrodes A1, A2 were discarded) and averaging across the counting Stroop trials for each type of stimulus. In Fig. 1, the

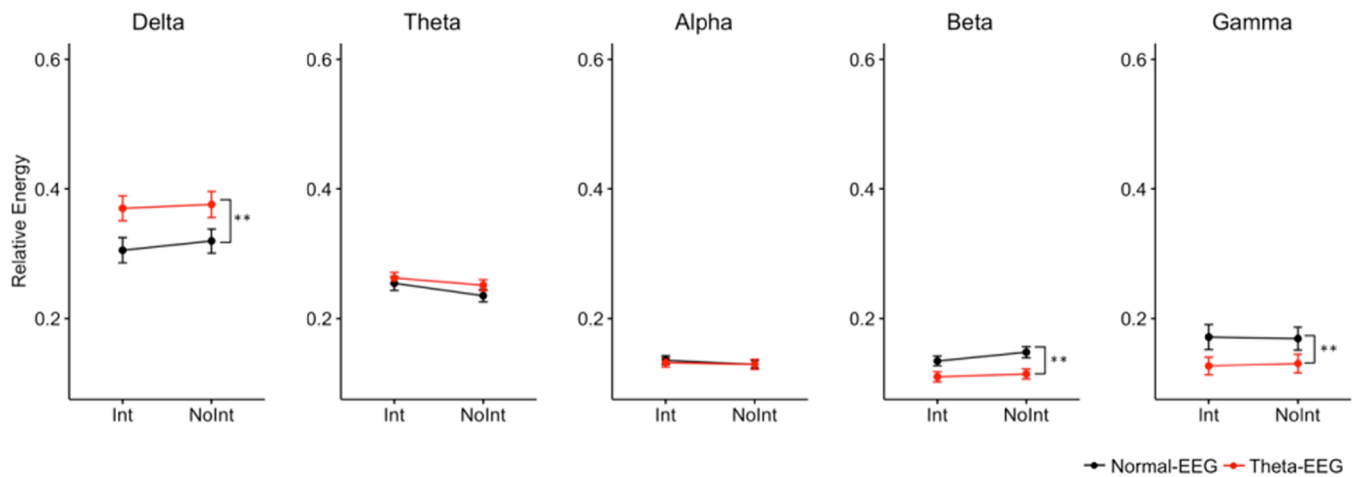


Fig. 3. Relative energy. Data are shown for each band according to the EEG group and to the type of stimulus. Data are expressed as means with standard error bars. ** $p < 0.01$ for group factor from two-way ANOVA.

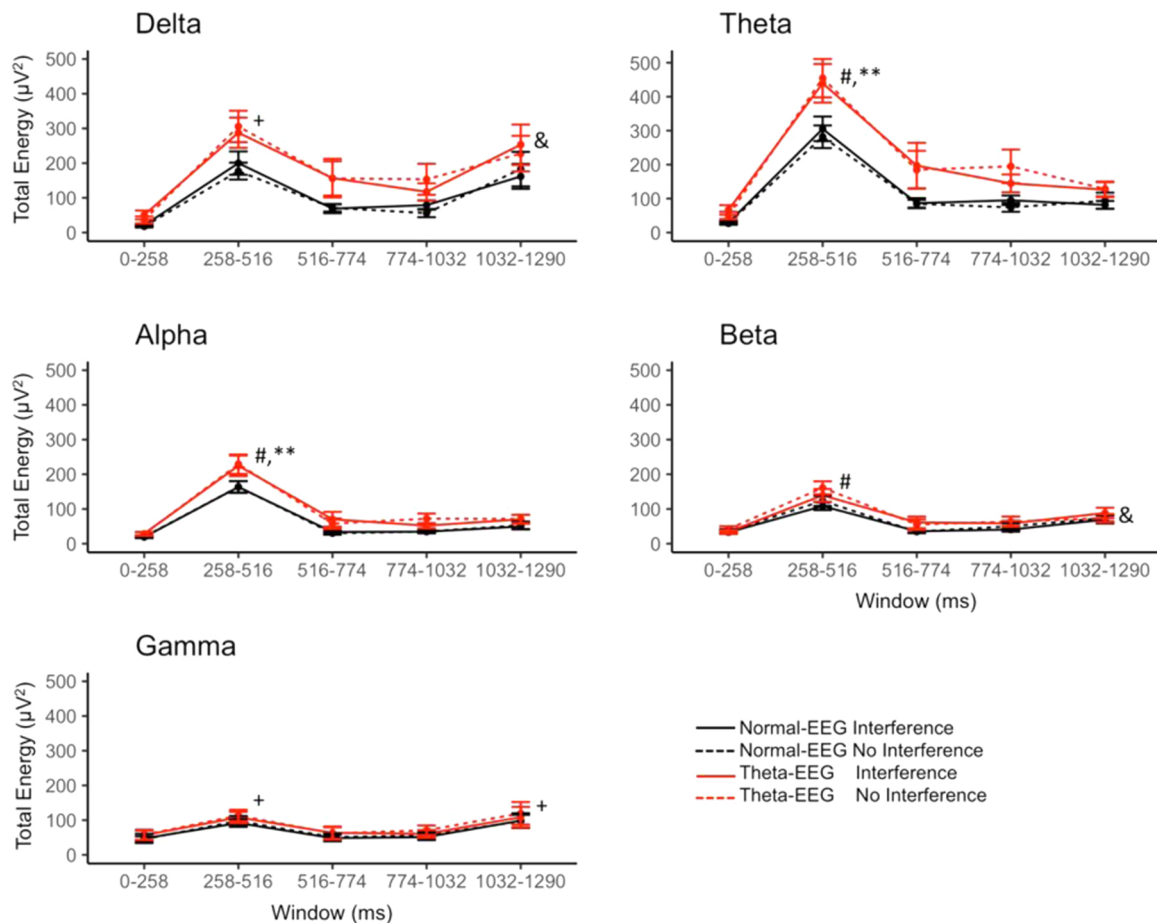


Fig. 4. Total energy for time windows and bands. Post hoc test of Group X Window: ** $p < 0.01$ between Normal-EEG and Theta-EEG for the 258–516 ms window. Post hoc test of Window: # $p < 0.05$ compared to the 0–258, 516–774, 774–1032, and 1032–1290 ms windows; + $p < 0.05$ compared to 0–258, 516–774, and 774–1032 ms windows; & $p < 0.05$ compared to 0–258 ms window. Data are expressed as means with standard error bars.

total energy for each group and stimulus type is shown for each frequency band. For delta band we found a main effect of Group ($F(1, 86) = 11.003, p = 0.00133$), while neither Stimulus ($F(1, 86) = 0.416, p = 0.51961$) nor the Group X Stimulus interaction were significant ($F(1, 86) = 0.036, p = 0.84973$). In theta band, there was a main effect of Group ($F(1, 86) = 11.605, p = 0.001$), while no significant differences were observed in Stimulus ($F(1, 86) = 0.031, p = 0.862$) or in the Group

X Stimulus interaction ($F(1, 86) = 0.01, p = 0.919$). Similarly, in alpha band there was a main effect of Group ($F(1, 86) = 8.539, p = 0.00444$), while Stimulus ($F(1, 86) = 0.002, p = 0.96375$) and the Group X Stimulus interaction remained without statistical significance ($F(1, 86) = 0.004, p = 0.95266$).

For beta band, neither Group ($F(1, 86) = 0.836, p = 0.363$) nor Stimulus ($F(1, 86) = 0.099, p = 0.753$) nor the Group X Stimulus

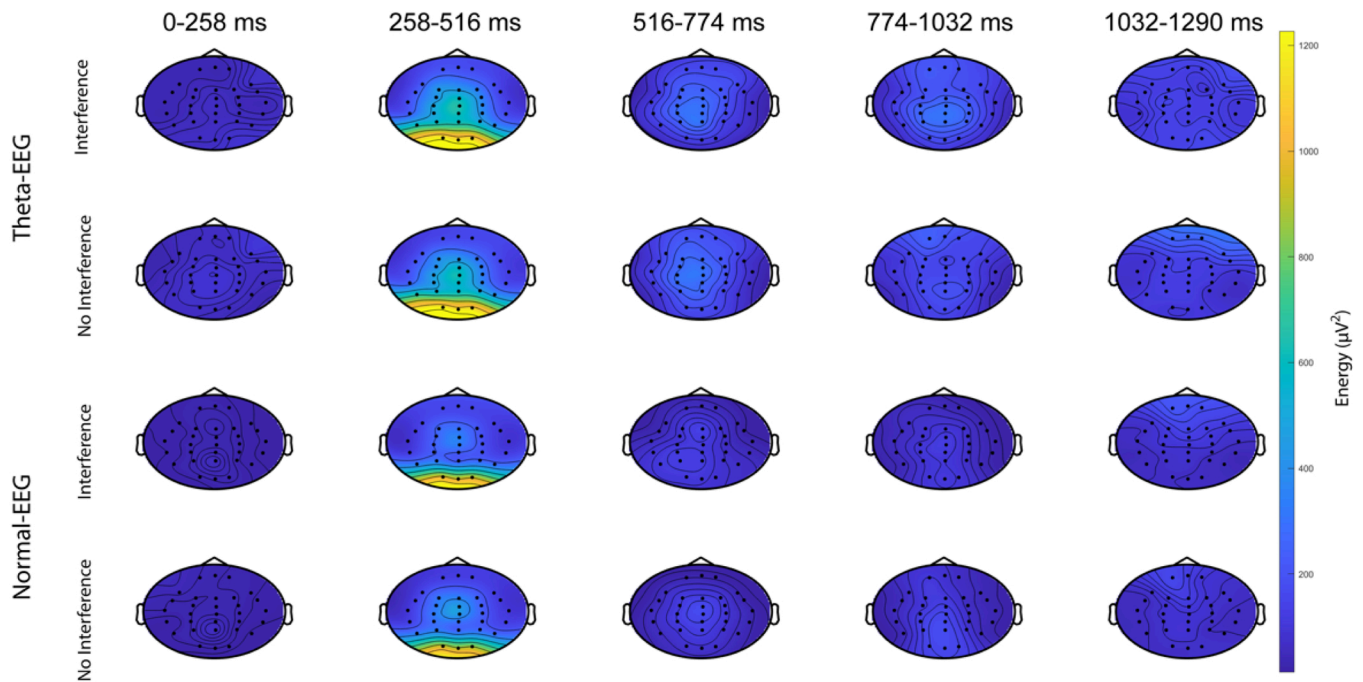


Fig. 5. Topographic distribution of the total energy in the theta band. Data are shown for each window and according to the group and type of stimulus. The color scale is expressed in μV^2 . (For interpretation of the references to colour in this figure, the reader is referred to the web version of this article.)

interaction were significant ($F(1, 86) = 0.078$, $p = 0.781$). Similar results were observed in gamma band, no significant differences were found for Group ($F(1, 86) = 0.330$, $p = 0.567$), Stimulus ($F(1, 86) = 0.127$, $p = 0.723$) or the Group X Stimulus interaction ($F(1, 86) = 0.027$, $p = 0.869$).

Overall, our analysis of the total energy showed a higher energy in the Theta-EEG group in delta, theta, and alpha bands irrespective of the type of stimulus presented during the counting Stroop task. In contrast, no significant differences in the total energy were observed in beta and gamma bands, as shown in Fig. 1.

In order to give visual intuition of energy distribution in the different frequency bands for each Stimulus and Group, we depicted in Fig. 2 the total energy across electrodes. We observed a higher total energy in Theta-EEG group than in Normal-EEG group in delta and theta bands. Although the reaction times between Interference and No Interference stimuli were different, this increase in total energy was similar for both types of stimuli. For delta band, the total energy increase was observed in the midline electrodes, while for theta band, this change was more pronounced in occipital electrodes. No obvious increase in total energy was visible in alpha, beta, and gamma bands.

3.3. Relative energy

In order to become independent of the total amount of energy among subjects, we further studied the relative wavelet energy for the entire signal. The relative energy corresponds to the amount of energy in each band, relative to the total energy aggregated for all frequency bands.

Fig. 3 shows the relative energy per frequency band for each group and stimulus type. In delta band we observed a main effect of Group ($F(1, 86) = 10.346$, $p = 0.00183$) but not of Stimulus ($F(1, 86) = 0.678$, $p = 0.41269$) or of the Group X Stimulus interaction ($F(1, 86) = 0.056$, $p = 0.81351$). In theta band neither of the variables nor the interaction between them were significant [Group ($F(1, 86) = 1.651$, $p = 0.202$); Stimulus ($F(1, 86) = 0.165$, $p = 0.686$); Group X Stimulus ($F(1, 86) = 0.186$, $p = 0.668$)]. For alpha band there were no statistical differences for any of the effects or the interaction between them [Group ($F(1, 86) = 0.070$, $p = 0.793$); Stimulus ($F(1, 86) = 0.021$, $p = 0.886$); Group

X Stimulus ($F(1, 86) = 0.062$, $p = 0.804$)].

The relative energy in beta band showed a main effect of Group ($F(1, 86) = 13.401$, $p = 0.000433$) but not for Stimulus ($F(1, 86) = 1.676$, $p = 0.198983$) or for the Group X Stimulus interaction ($F(1, 86) = 0.312$, $p = 0.577787$). Similarly, for the gamma band, there was a main effect of Group ($F(1, 86) = 7.017$, $p = 0.00961$), but no differences were observed for Stimulus ($F(1, 86) = 0.259$, $p = 0.61188$) or for the Group X Stimulus interaction ($F(1, 86) = 0.038$, $p = 0.84581$).

Our analysis therefore revealed that even after normalizing by the total amount of energy used during the task, the Theta-EEG group showed an increase of relative energy in the delta band, as compared to the Normal-EEG group, which was independent of the type of stimulus presented. Moreover, a decrease in relative energy was observed in beta and gamma bands.

3.4. Total energy across windows

To analyze the signal in the temporal domain, we took time windows of at least $2^7 + 1 = 129$ points, which corresponded to 258 ms; this procedure allowed us to analyze five-time windows in the ERP signal. The energy across electrodes was averaged. Fig. 4 shows the total energy per window. For the delta band, significant main effects of Group ($F(1, 430) = 21.058$, $p = 5.86 \times 10^{-6}$) and Window ($F(4, 430) = 12.610$, $p = 1.04 \times 10^{-9}$) were observed, but there were not significant effects of Stimulus ($F(1, 430) = 0.149$, $p = 0.7$) or the interaction among factors [Group X Stimulus ($F(1, 430) = 0.062$, $p = 0.804$); Group X Window ($F(4, 430) = 0.79$, $p = 0.532$); Stimulus X Window ($F(4, 430) = 0.307$, $p = 0.873$); Group X Stimulus X Window ($F(4, 430) = 0.367$, $p = 0.832$)]. The analysis of the Window factor showed that the total energy in the 258–516 ms window was higher than in the windows 0–258, 516–774, and 774–1032 ms ($p \leq 0.03783$ for each comparison). For this same band, the total energy in the 1032–1290 ms window was higher than in the window 0–258 ms ($p = 0.00893$).

For the theta band, there were significant main effects of Group ($F(1, 430) = 30.596$, $p = 5.53 \times 10^{-8}$) and Window ($F(4, 430) = 17.546$, $p = 2.38 \times 10^{-13}$) but not of Stimulus ($F(1, 430) = 0.279$, $p = 0.5978$). The interaction Group X Window was close to significance ($F(4, 430)$

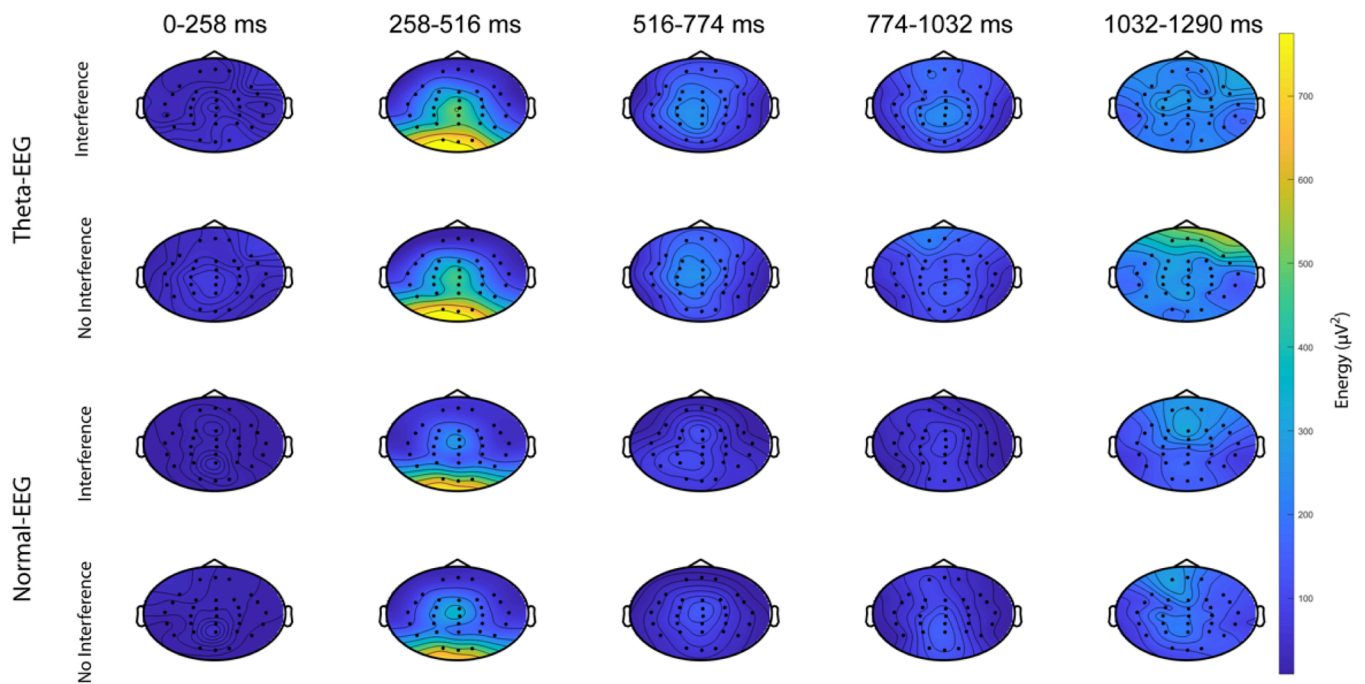


Fig. 6. Topographic distribution of the total energy in the delta band. Data are shown for each window and according to the group and type of stimulus. The color scale is expressed in μV^2 . (For interpretation of the references to colour in this figure, the reader is referred to the web version of this article.)

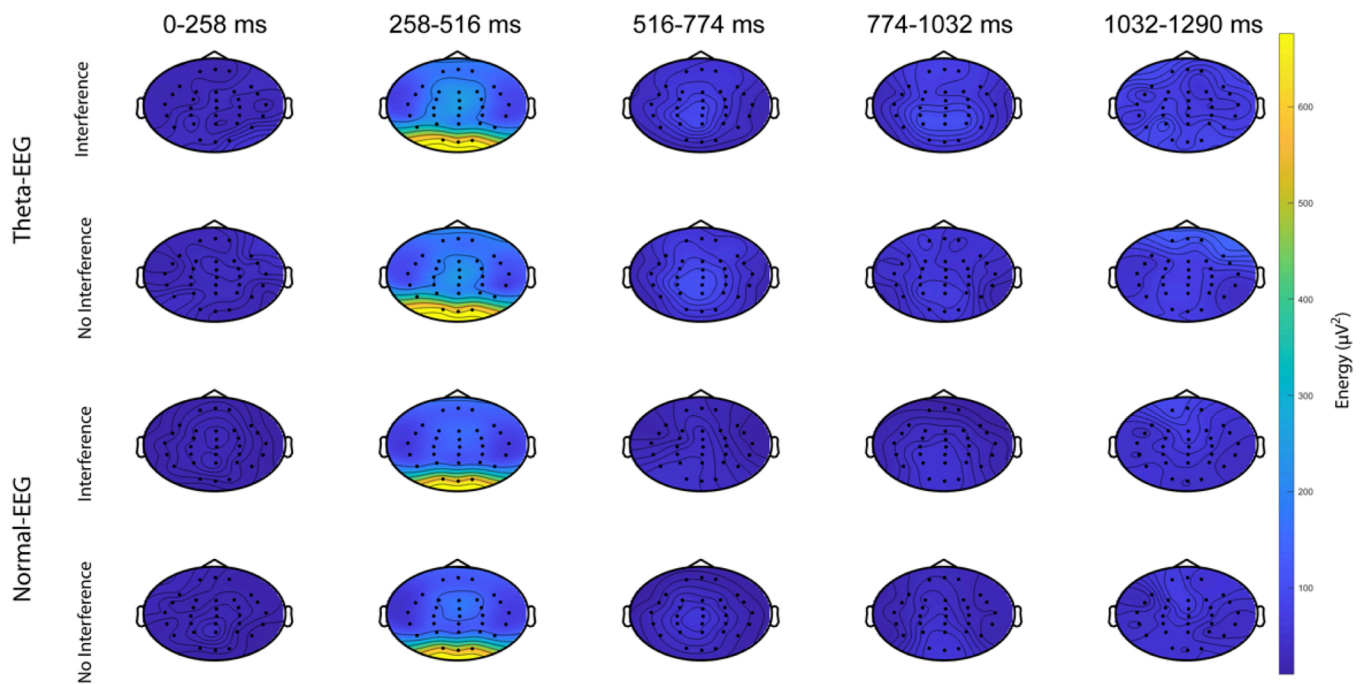


Fig. 7. Topographic distribution of the total energy in the alpha band. Data are shown for each window and according to the group and type of stimulus. The color scale is expressed in μV^2 . (For interpretation of the references to colour in this figure, the reader is referred to the web version of this article.)

$= 2.229$, $p = 0.0651$), while the other interactions were not significant [Group X Stimulus ($F(1, 430) = 0.241$, $p = 0.624$); Stimulus X Window ($F(4, 430) = 0.298$, $p = 0.8794$); Group X Stimulus X Window ($F(4, 430) = 0.321$, $p = 0.8639$)]. The analysis of the Window factor showed that the total energy in the 258–516 ms window was higher than in all the other windows ($p < 0.0001$ for all the comparisons). As is depicted in Fig. 4, the post hoc test for the interaction Group X Window indicated that the total energy in the 258–516 ms window was higher in the Theta-EEG group when compared to the Normal-EEG group ($p = 0.0065$).

For the alpha band, the total energy showed significant main effects of Group ($F(1, 430) = 23.548$, $p = 1.71 \times 10^{-6}$) and Window ($F(4, 430) = 34.484$, $p < 2 \times 10^{-16}$), while Stimulus was not significant ($F(1, 430) = 0.005$, $p = 0.9452$). The interaction Group X Window was close to statistical significance ($F(4, 430) = 2.163$, $p = 0.0724$), while other interactions did not show significant differences [Group X Stimulus ($F(1, 430) = 0.03$, $p = 0.8622$); Stimulus X Window ($F(4, 430) = 0.053$, $p = 0.9947$); Group X Stimulus X Window ($F(4, 430) = 0.149$, $p = 0.9633$)]. The analysis of the Window factor showed that the total

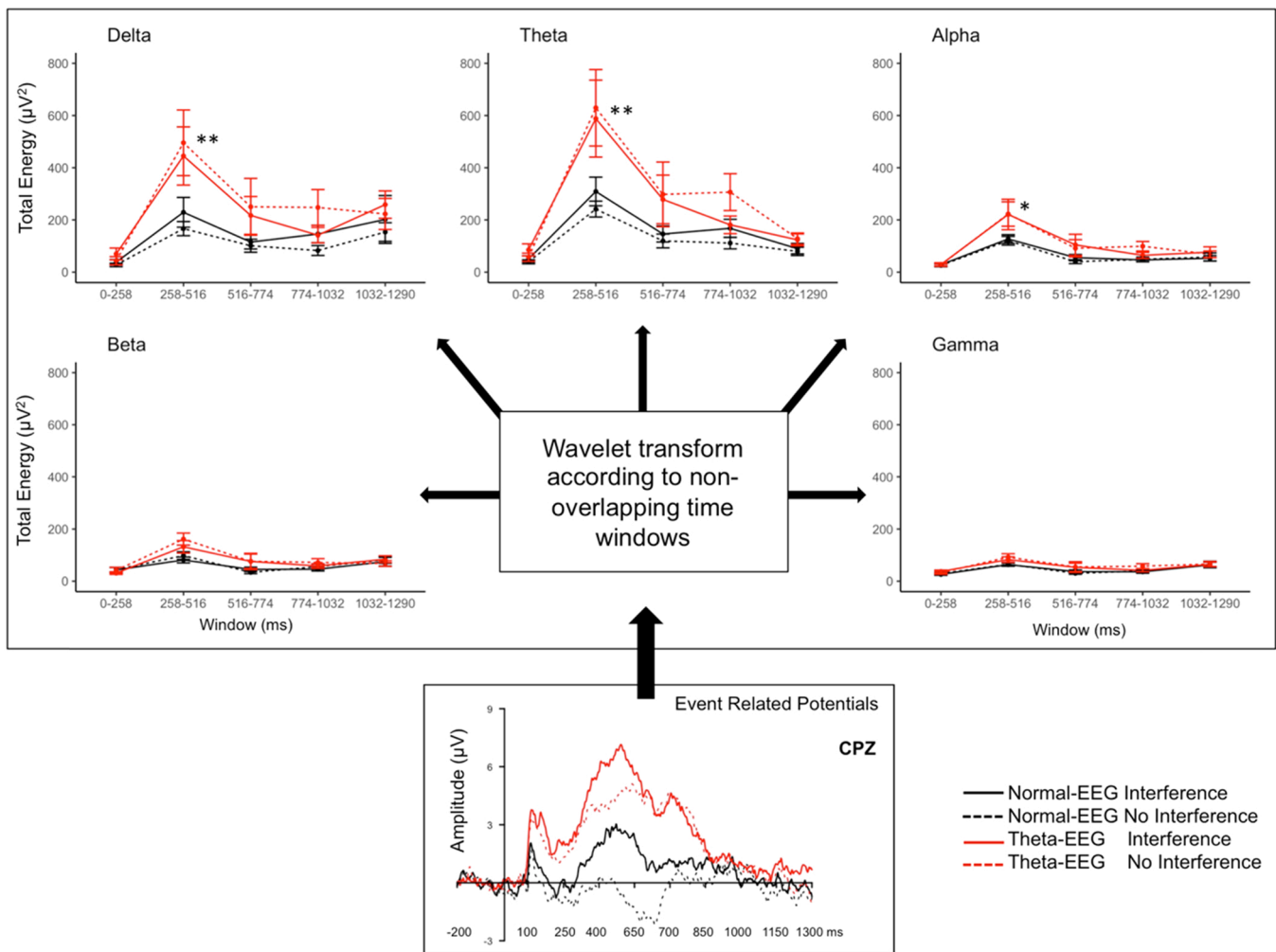


Fig. 8. Total energy in the CPZ electrode. The amplitude of the signal obtained by event-related potentials during a counting Stroop task was further analyzed by wavelet transform. $**p < 0.01$, $*p < 0.05$ for the 258–516 ms window when comparing Theta-EEG versus Normal-EEG in the post hoc analysis of the interaction Group X Window. No significant differences were observed for other windows or for the type of stimulus.

energy in the 258–516 ms window was higher than in all the other windows ($p < 0.0001$ for each comparison). The analysis of the interaction Group X Window indicated that the total energy in the 258–516 ms window was higher in the Theta-EEG group than in the Normal-EEG group ($p = 0.0079$), Fig. 4.

For beta band we found significant main effects of Group ($F(1, 430) = 10.868$, $p = 0.00106$) and Window ($F(4, 430) = 17.402$, $p = 3.03 \times 10^{-13}$), while there were no statistical differences for Stimulus ($F(1, 430) = 0.311$, $p = 0.57723$). None of the interactions of the factors was significant either [Group X Stimulus ($F(1, 430) = 0.105$, $p = 0.74663$); Group X Window ($F(4, 430) = 1.046$, $p = 0.3829$); Stimulus X Window ($F(4, 430) = 0.295$, $p = 0.88137$); Group X Stimulus X Window ($F(4, 430) = 0.2$, $p = 0.93804$)]. The post hoc comparisons of the Window factor showed that the total energy in the 258–516 ms window was higher than in all the other windows ($p \leq 0.0143$ for all the comparisons). Additionally, the energy in the 1032–1290 ms window was higher than in the 0–258 ms window ($p = 0.0261$), as shown in Fig. 4.

Finally, the analysis of total energy in the gamma band revealed a significant main effect of Window ($F(4, 430) = 4.018$, $p = 0.00328$), while Group ($F(1, 430) = 3.242$, $p = 0.07246$) and Stimulus ($F(1, 430) = 0.318$, $p = 0.57321$) did not reach significance. None of the interactions among factors was significant [Group X Stimulus ($F(1, 430) = 0.053$, $p = 0.81849$); Group X Window ($F(4, 430) = 0.021$, $p = 0.99915$); Stimulus X Window ($F(4, 430) = 0.093$, $p = 0.98453$);

Group X Stimulus X Window ($F(4, 430) = 0.037$, $p = 0.99741$)]. The analysis of the Window factor showed that the total energy in the 258–516 ms window was higher than in the windows 0–258, 516–774, and 774–1032 ms ($p < 0.01$ for all comparisons). The total energy in the 1032–1290 ms window was also higher than that observed in the windows 0–258, 516–774, and 774–1032 ms ($p \leq 0.002$ for all comparisons), as shown in Fig. 4.

Overall, our analysis across windows revealed a higher amount of total energy in the Theta-EEG group than in the Normal-EEG group in the delta, theta, alpha, and beta bands irrespective of the type of stimulus presented. For theta and alpha bands, the total energy was higher in the Theta-EEG group than in the Normal-EEG group, specifically for the 258–516 ms window, as depicted in Fig. 4.

To provide visual intuition of the energy changes on each electrode occurring across windows we generated topographical maps for theta, delta, and alpha bands. Fig. 5 shows the topographical distribution of the energy in theta band per group and type of stimulus through time. The topographic distribution of the total energy across windows for theta band corroborated the relevance of the 258–516 ms window found in the analysis shown in Fig. 4.

The topographic map of theta band showed a higher total energy in the Theta-EEG group as compared to the Normal-EEG group only in the 258–516 ms window. The amount of total energy looked similar for both types of stimuli in the same EEG group. The increased energy for this theta band in the Theta-EEG group was more prominent in mid-line and

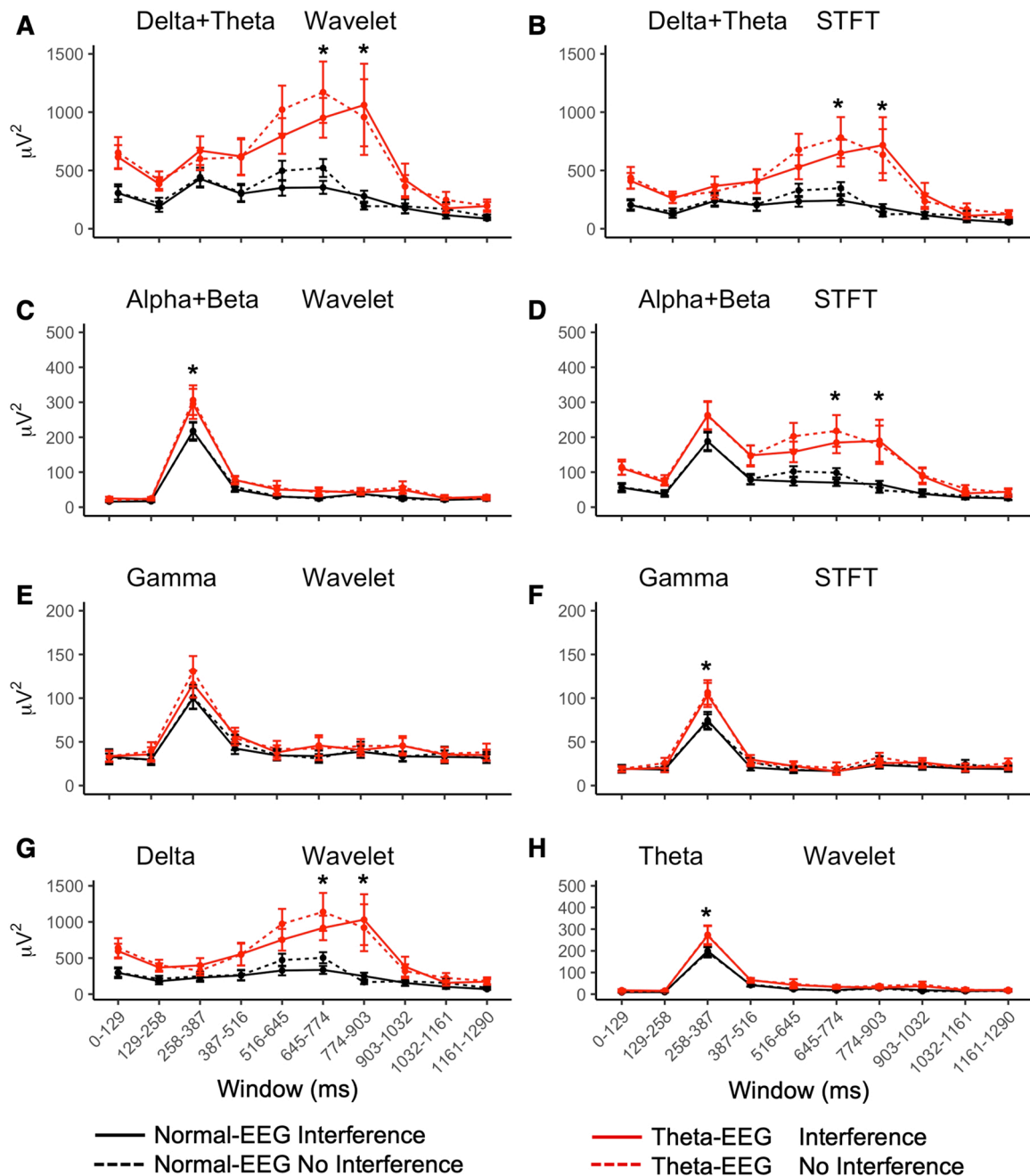


Fig. 9. Wavelet and Short Time Fourier Transform analyses across ten windows. (A-B) Delta+Theta energy obtained by wavelet or STFT analysis. (C-D) Alpha+Beta energy obtained by wavelet or STFT analysis. (E) Gamma energy obtained by wavelets. (F) Gamma energy obtained by STFT. (G) Delta energy obtained by wavelets. (H) Theta energy obtained by wavelets. Post hoc test of Group X Window: * $p < 0.05$ between Normal-EEG and Theta-EEG for the indicated window. Data are expressed as means with standard error bars.

occipital electrodes (Fig. 5). Similar changes were observed in delta and alpha bands (Figs. 6 and 7): increased total energy for both types of stimuli in the Theta-EEG group was observed in mid-line and occipital electrodes towards frontal regions; this change was prominent in the 258–516 ms window.

3.5. Wavelet analysis on central electrodes

The changes observed in the topographic maps (Figs. 5–7) led us to further inspect specific midline electrodes. As shown in Fig. 8, we performed an analysis for central electrodes to better depict the information added by wavelet analysis when studying the data obtained by ERP.

The wavelet transform of the voltage in the CPZ electrode showed a

significant Group X Window interaction in delta, theta, and alpha bands in the total energy (Table 1, Appendix B). The post hoc test indicated that the total energy was higher in the Theta-EEG group than in the Normal-EEG group in the 258–516 ms window for the three bands ($p \leq 0.0141$). The differences in total energy for CPZ electrode in delta, theta, and alpha bands were independent of the type of stimulus presented (Stimulus, Group X Stimulus, Stimulus X Window, and Group X Stimulus X Window were not significant; Table 1, Appendix B). Although the Group X Window interaction was significant for the beta band (Table 1, Appendix B), the post hoc comparison did not show any statistical difference between Theta-EEG and Normal-EEG conditions for any given window ($p \geq 0.0720$). For the gamma band, there was a significant effect of Group and Window, but not for other factors or

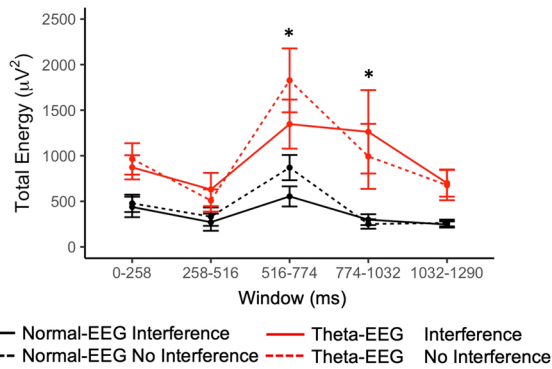


Fig. 10. Slow wave band energy using five windows. The [0, 1.9531] Hz band was analyzed. Post hoc test of Group X Window: *p < 0.05 between Normal-EEG and Theta-EEG for the indicated windows.

interactions (Table 1, Appendix B).

The total energy in the PZ electrode showed a significant Group X Window interaction for the delta, and theta bands (Table 1, Appendix B). The total energy was higher in the Theta-EEG group for the 258–516 ms window ($p \leq 0.0005$ for delta and theta bands). In the alpha, beta, and gamma bands, only the factors Group and Window showed statistical significance (Table 1, Appendix B).

A similar increase in the total energy in the alpha band was observed in FCZ and CZ electrodes for the Theta-EEG group. There was a significant Group X Window interaction in the alpha band for both electrodes (Table 1, Appendix B). The total energy was higher in the Theta-EEG group than in the Normal-EEG group only in the 258–516 ms window (FCZ $p = 0.0288$; CZ $p = 0.0175$). For the CZ electrode, the Group X Window interaction was significant for the beta band; however, the post hoc comparisons did not reveal statistical differences for any specific time window (Table 1, Appendix B). For FCZ and CZ electrodes, only the factors Group and Window showed statistical significance for delta, theta, and gamma bands (Table 1, Appendix B).

Taken together, our analysis of wavelet transform for central

electrodes indicated that the total energy was higher in the Theta-EEG group than in the Normal-EEG group in the 258–516 ms window in the delta and theta bands for more posterior electrodes (CPZ, PZ). The increase in total energy in the Theta-EEG group was observed in the 258–516 ms window for the alpha band in more anterior electrodes (FCZ, CZ).

3.6. Comparison with short time fourier transform

Our previous wavelet analysis showed that the energy in delta, theta, and alpha bands was highly increased during a Stroop task in elderly with excess in theta activity in their resting EEG. We next deemed important to evaluate the changes in these bands with another signal processing method. Time-frequency analysis applied to ERPs can also be performed by using a Short Time Fourier Transform (STFT). To stress the similarities and differences between wavelet transform and STFT, we calculated the total energy using ten time windows. In this case, the differentiation between delta and theta bands and between alpha and beta bands is not possible with STFT (as mentioned in Section 2.5). Therefore, to achieve a direct comparison between wavelets and STFT, we analyzed delta+theta bands and alpha+beta bands (Fig. 9 A-D). For the wavelet analysis we found significant effects of Group, Window, and Group X Window in the delta+theta energy [Group ($F(1, 860) = 71.992, p = 2.0 \times 10^{-16}$); Window ($F(4, 860) = 4.77, p < 3.2 \times 10^{-6}$); Group X Window ($F(4, 860) = 3.516, p = 0.000274$)]. The analysis of the interaction Group X Window indicated that the energy signal in the 645–774 ms and in the 774–903 ms windows was higher in the Theta-EEG group than in the Normal-EEG group ($p < 0.009$ for both windows) (Fig. 9 A). When using STFT, we found very similar results; Group, Window, and Group X Window showed significant differences [Group ($F(1, 860) = 68.585, p = 4.63 \times 10^{-16}$); Window ($F(4, 860) = 4.557, p = 6.9 \times 10^{-6}$); Group X Window ($F(4, 860) = 3.667, p = 0.000162$)] and the analysis of the interaction Group X Window indicated that the voltage in the delta+theta band in the 645–774 ms and in the 774–903 ms windows was higher in the Theta-EEG group than in the Normal-EEG group ($p < 0.009$ for both windows) (Fig. 9 B).

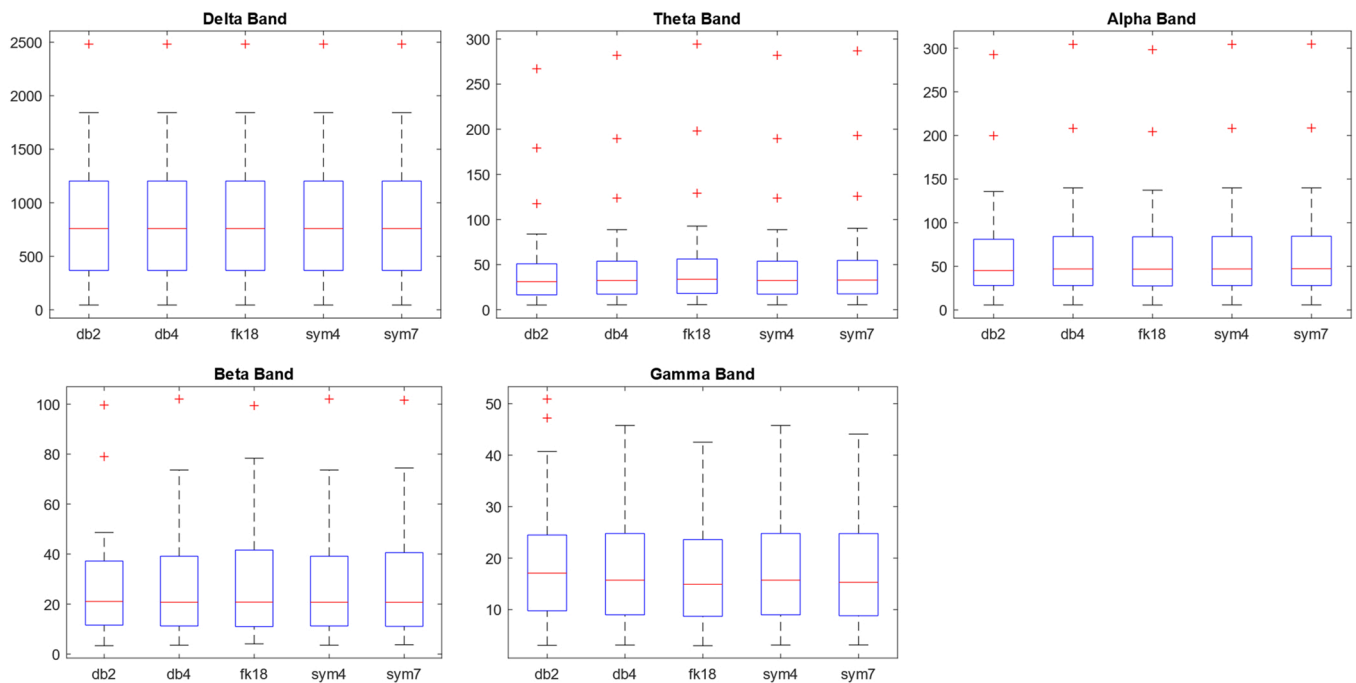


Fig. A1. Different mother wavelets used in the calculation of the total energy averaged across electrodes. Data correspond to the Interference condition in the Theta-EEG group for the 0–258 ms window. Wavelet Daubechies2 (db2), WaveletDaubechies4 (db4), Fejér-Korovkin wavelet (fk18), Wavelet Symlets 4 and Wavelet Symlets 7. (A) Delta Band. (B) Theta Band. (C) Alfa Band. (D) Beta band. (E) Gamma Band.

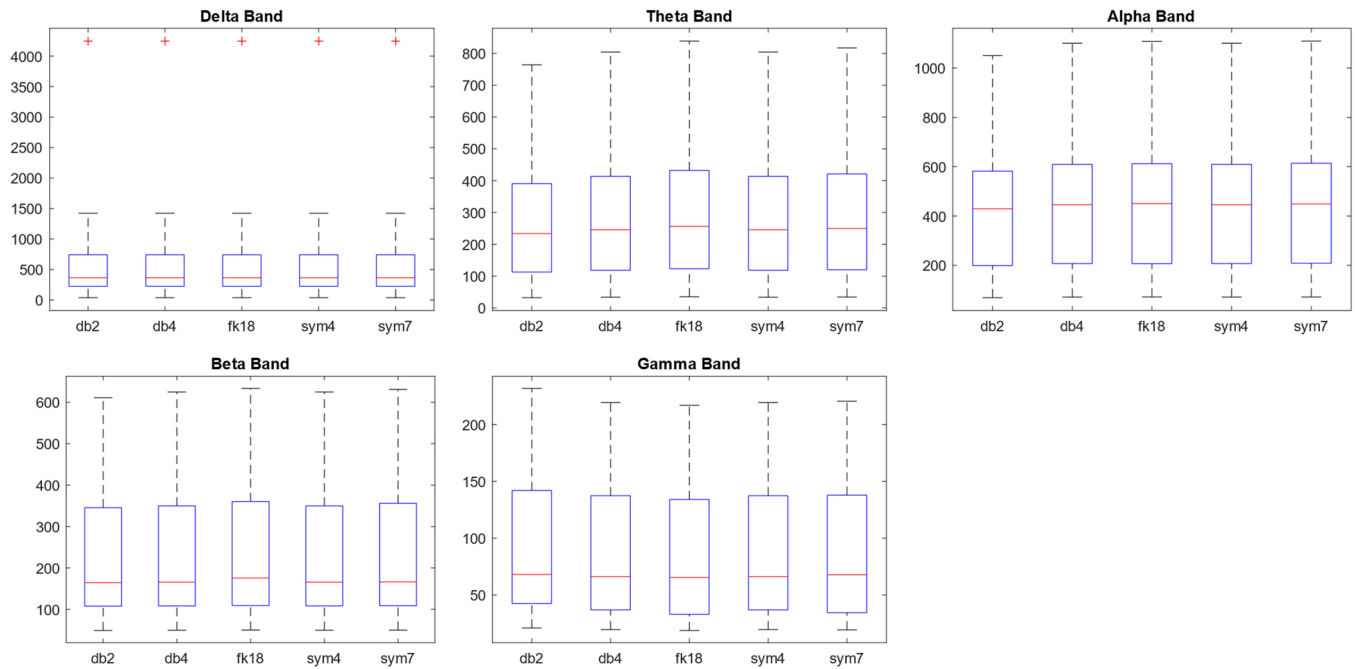


Fig. A2. Different mother wavelets used in the calculation of the total energy averaged across electrodes. Data correspond to the Interference condition in the Theta-EEG group for the 258–516 ms window. Wavelet Daubechies 2 (db2), Wavelet Daubechies 4 (db4), Fejér-Korovkin wavelet (fk18), Wavelet Symlets 4 and Wavelet Symlets 7. (A) Delta Band. (B) Theta Band. (C) Alfa Band. (D) Beta band. (E) Gamma Band.

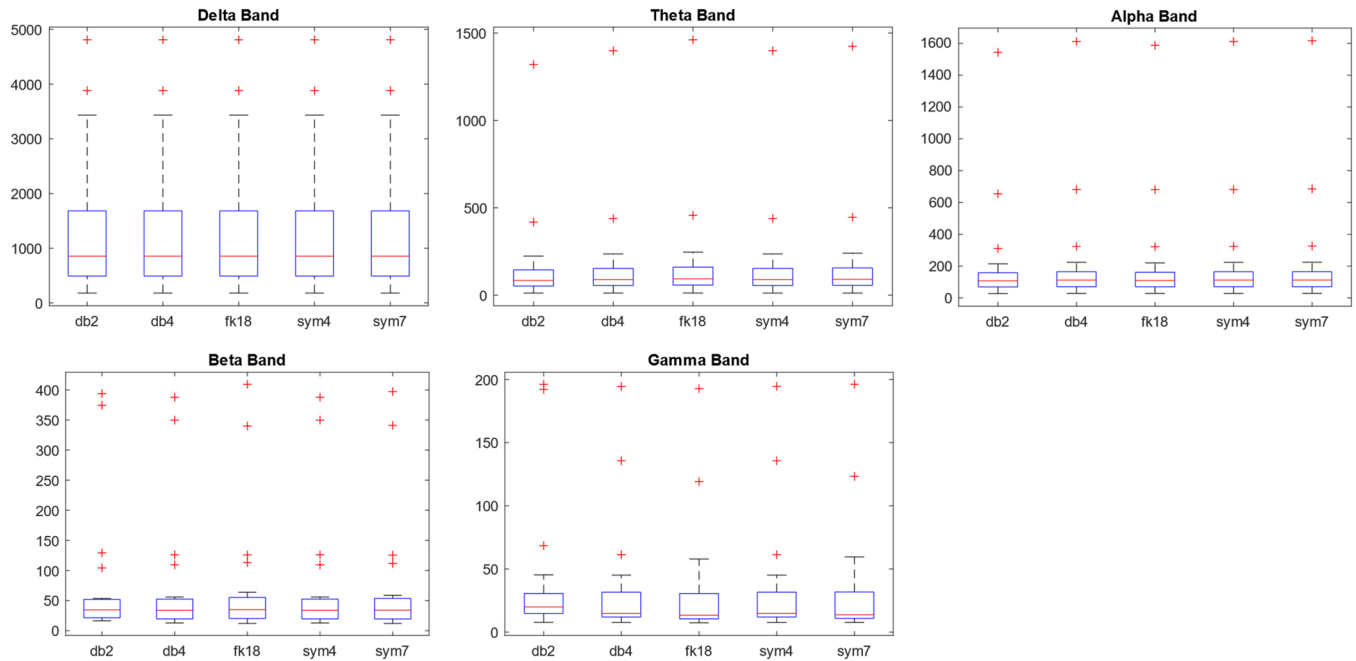


Fig. A3. Different mother wavelets used in the calculation of the total energy averaged across electrodes. Data correspond to the Interference condition in the Theta-EEG group for the 516–774 ms window. Wavelet Daubechies 2 (db2), Wavelet Daubechies 4 (db4), Fejér-Korovkin wavelet (fk18), Wavelet Symlets 4 and Wavelet Symlets 7. (A) Delta. (B) Theta Band. (C) Alfa Band. (D) Beta band. (E) Gamma Band.

When exploring alpha+beta bands with wavelets we found significant differences in Group, Window, and Group X Window [Group ($F(1, 860) = 22.816, p = 2.1 \times 10^{-6}$); Window ($F(4, 860) = 37.834, p < 2 \times 10^{-16}$); Group X Window ($F(4, 860) = 3.189, p = 0.000835$)]. The analysis of the Group X Window interaction revealed that the energy in the Theta-EEG group was higher than the energy in the Normal-EEG group only in the 258–387 ms window ($p = 0.0001$) (Fig. 9 C). With STFT we found that also Group, Window, and Group X Window were

statistically significant [Group ($F(1, 860) = 76.629, p < 2 \times 10^{-16}$); Window ($F(4, 860) = 8.331, p = 5.68 \times 10^{-12}$); Group X Window ($F(4, 860) = 2.623, p = 0.0054$)]. The post hoc analysis of Group X Window showed that there were differences between groups in the 645–774 ms and in the 774–903 ms windows ($p < 0.05$ for both comparisons) (Fig. 9 D).

The wavelet analysis of gamma band with ten windows revealed differences only in Group and Window [Group ($F(1, 860) = 8.135,$

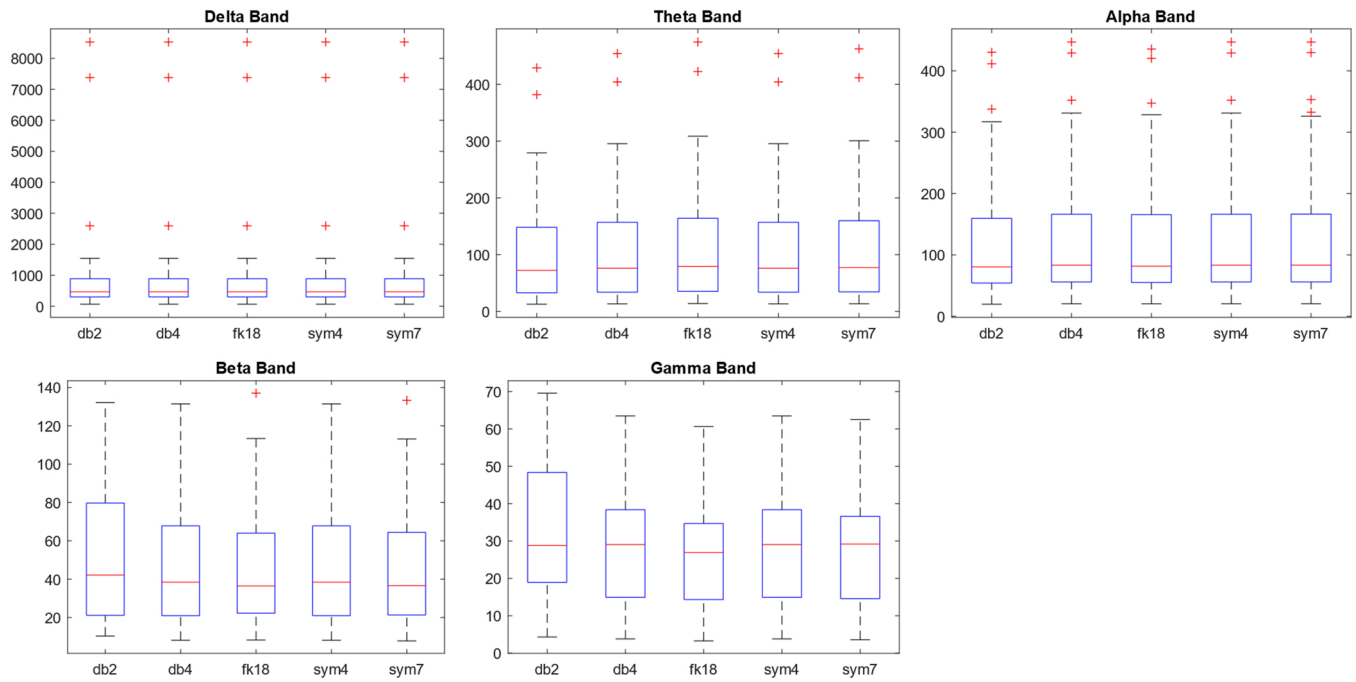


Fig. A4. Different mother wavelets used in the calculation of the total energy averaged across electrodes. Data correspond to the Interference condition in the Theta-EEG group for the 774–1032 ms window. Wavelet Daubechies 2 (db2), Wavelet Daubechies 4 (db4), Fejér-Korovkin wavelet (fk18), Wavelet Symlets 4 and Wavelet Symlets 7. (A) Delta Band. (B) Theta Band. (C) Alfa Band. (D) Beta band. (E) Gamma Band.

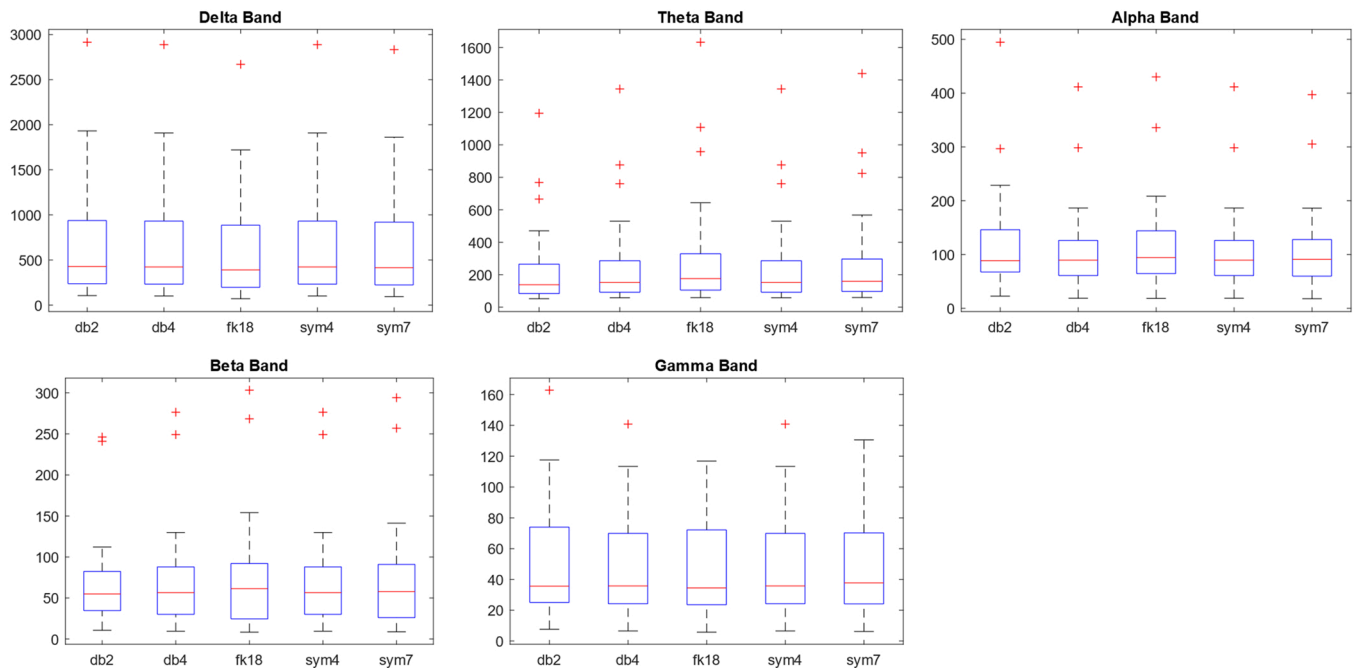


Fig. A5. Different mother wavelets used in the calculation of the total energy averaged across electrodes. Data correspond to the Interference condition in the Theta-EEG group for the 1032–1290 ms window. Wavelet Daubechies 2 (db2), Wavelet Daubechies 4 (db4), Fejér-Korovkin wavelet (fk18), Wavelet Symlets 4 and Wavelet Symlets 7. (A) Delta Band. (B) Theta Band. (C) Alfa Band. (D) Beta band. (E) Gamma Band.

$p = 0.00445$); Window ($F(4, 860) = 8.515$ $p = 2.84 \times 10^{-12}$)] however the Group X Window was not significant ($F(4, 860) = 0.581$, $p = 0.81361$) (Fig. 9 E). With STFT we observed significant effects of Group, Window, and Group X Window [Group ($F(1, 860) = 9.648$, $p = 0.00196$); Window ($F(4, 860) = 17.684$, $p < 2 \times 10^{-16}$); Group X Window ($F(4, 860) = 2.84$, $p = 0.00266$)]. The post hoc analysis of Group X Window revealed that the energy in gamma band was higher in

the Theta-EEG group only in the 258–387 ms window ($p = 0.004$) (Fig. 9 F).

The properties of the wavelet transform allow us to examine separately delta and theta bands across the ten windows. This could not be achieved using STFT, due to its fixed time-frequency resolution independently of the frequency range considered. The range of the bands were the following: for delta between $[0, 3.9063)$ Hz and for theta

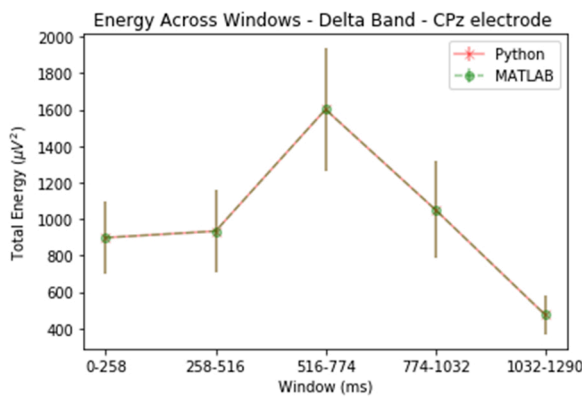


Fig. A6. The results using the STFT function implemented in Python and MATLAB.

between [3.9063, 7.8125] Hz. In the delta band we observed that Group, Window, and Group X Window showed significant differences [Group (F(1, 860)= 66.876, p = 1.03 × 10⁻¹⁵); Window (F(4, 860)= 4.829 p = 2.58 × 10⁻⁶); Group X Window (F(4, 860) = 3.78, p = 0.000109)]. The post hoc analysis of Group X Window indicated that the energy in the 645–774 ms and in the 774–903 ms windows was higher in the Theta-EEG group than in the Normal-EEG group (p < 0.009 for both windows) (Fig. 9 G). When analyzing the theta band we found that Group, Window, and Group X Window factor were significant [Group (F(1, 860)= 20.966, p = 5.37 × 10⁻⁶); Window (F(4, 860)= 36.082 p < 2 × 10⁻⁶); Group X Window (F(4, 860) = 2.944, p = 0.00189)]. The analysis of Group X Window interaction revealed that Theta-EEG and Normal-EEG group were only different in the 258–387 ms window (p = 0.00017) (Fig. 9 H).

Altogether, using wavelet or STFT we showed that the energy in delta+theta and alpha+beta bands is increased in the Theta-EEG group during a Stroop task and that this change is independent of stimulus type. With wavelet analysis we were further able to show that the

increase in delta energy in the Theta-EEG group occurred between 645 and 903 ms while the increase in theta energy was visible in the 258–387 ms window.

To compare the reliability of the analysis made using Matlab to apply wavelet analysis, we performed the analysis in Python using the standard python package scipy.signal (Appendix A, Fig. A.6).

3.6.1. Slow wave activity

When exploring ten windows by wavelets the results obtained in the delta band (Fig. 9 G) contrast with the results of five windows using the same methodology (Figs. 4 and 8). This difference may have relied on the frequency band ranges used as with ten windows the range was [0, 3.9063] Hz and with 5 windows we used [1.9531–3.9063] Hz. To confirm this, we evaluated the total energy averaged across electrodes for the [0, 1.9531] Hz range using five windows. The Group and Window factor showed significant differences [Group (F(1, 430)= 45.191, p = 5.7 × 10⁻¹¹); Window (F(4, 430)= 3.126 p = 0.0149)] while the interaction Group X Window was close to significance (F(1, 430)= 1.975, p = 0.0975). The post hoc analysis of the interaction Group X Window showed that there were differences between Theta-EEG and Normal-EEG groups in the 526–774 and 774–1032 ms windows (p < 0.05 for both comparisons). This result confirmed that the increase in energy in the delta band in the Theta-EEG group occurred between 516 and 1032 ms for the [0, 1.9531] Hz frequency and between 258 and 516 ms for the [1.9531–3.9063] Hz frequency.

4. Discussion

By using a wavelet analysis, we aimed to explore whether the EEG signal energy obtained from ERP during a counting Stroop task was different between a group of elderly subjects with excess of theta activity in their EEG and another one with normal EEG. The methods applied in the present study complement ERP analysis used in similar studies involving the elderly. With wavelets we were able to discern that the major difference in theta and alpha energy was in the window

Table B1

Two-way ANOVA results for the total energy in central electrodes.

| Electrode | Band/ ANOVA factors | Delta | Theta | Alpha | Beta | Gamma |
|-----------|---------------------------|--------------------------------|--------------------------------|--------------------------------|--------------------------------|-------------------------------|
| | | F (1, 430); p-value | F (1, 430); p-value | F (1, 430); p-value | F (1, 430); p-value | F (1, 430); p-value |
| FCZ | Group | 9.1; 0.003 | 12.5; 0.0004 | 12.5; 0.0004 | 7.1; 0.008 | 4.2; 0.04 |
| | Stimulus | 0.003; 0.9 | 0.3; 0.6 | 0.006; 0.9 | 1.5; 0.2 | 0.8; 0.4 |
| | Window | 5.9; 0.0001 | 9.7; 1.54 × 10 ⁻⁰⁷ | 19.2; 1.64 × 10 ⁻¹⁴ | 13.0; 5.21 × 10 ⁻¹⁰ | 7.4; 8.72 × 10 ⁻⁰⁶ |
| | Group X Stimulus | 0.2; 0.7 | 0.6; 0.4 | 0.3; 0.6 | 0.3; 0.6 | 0.09; 0.8 |
| | Group X Window | 0.5; 0.8 | 1.3; 0.3 | 2.4; 0.05 | 2.0; 0.1 | 0.4; 0.8 |
| | Stimulus X Window | 1.0; 0.4 | 0.5; 0.7 | 0.2; 0.97 | 0.8; 0.5 | 0.9; 0.4 |
| CZ | Group X Stimulus X Window | 0.4; 0.8 | 0.4; 0.8 | 0.3; 0.9 | 0.4; 0.8 | 0.4; 0.8 |
| | Group | 11.7; 0.0007 | 14.6; 0.0002 | 12.8; 0.0004 | 6.5; 0.01 | 6.2; 0.01 |
| | Stimulus | 0.1; 0.8 | 0.2; 0.6 | 0.01; 0.9 | 1.3; 0.3 | 0.7; 0.4 |
| | Window | 5.6; 0.0002 | 9.5; 2.42 × 10 ⁻⁰⁷ | 16.9; 6.73 × 10 ⁻¹³ | 12.9; 6.49 × 10 ⁻¹⁰ | 8.7; 9.07 × 10 ⁻⁰⁷ |
| | Group X Stimulus | 1.1; 0.3 | 1.1; 0.3 | 0.2; 0.7 | 0.01; 0.9 | 0.1; 0.7 |
| | Group X Window | 0.9; 0.5 | 1.8; 0.1 | 2.6; 0.03 | 2.4; 0.05 | 0.5; 0.8 |
| CPZ | Stimulus X Window | 0.6; 0.6 | 0.6; 0.7 | 0.1; 0.97 | 0.4; 0.8 | 1.1; 0.4 |
| | Group X Stimulus X Window | 0.4; 0.8 | 0.4; 0.8 | 0.2; 0.99 | 0.3; 0.9 | 0.3; 0.9 |
| | Group | 16.9; 4.62 × 10 ⁻⁰⁵ | 20.8; 6.75 × 10 ⁻⁰⁶ | 15.2; 0.0001 | 8.2; 0.005 | 9.3; 0.002 |
| | Stimulus | 0.3; 0.61 | 0.3; 0.6 | 0.02; 0.9 | 0.8; 0.4 | 0.3; 0.6 |
| | Window | 4.5; 0.001 | 8.5; 1.40 × 10 ⁻⁰⁶ | 16.2; 2.8 × 10 ⁻¹² | 11.9; 3.45 × 10 ⁻⁰⁹ | 8.8; 8.3e X10 ⁻⁰⁷ |
| | Group X Stimulus | 1.4; 0.2 | 1.3; 0.3 | 0.2; 0.8 | 0.04; 0.8 | 0.2; 0.6 |
| PZ | Group X Window | 2.5; 0.0447 | 3.7; 0.006 | 2.7; 0.03 | 3.1; 0.02 | 0.9; 0.5 |
| | Stimulus X Window | 0.5; 0.8 | 0.4; 0.8 | 0.1; 0.98 | 0.2; 0.95 | 0.96; 0.4 |
| | Group X Stimulus X Window | 0.4; 0.8 | 0.4; 0.8 | 0.1; 0.97 | 0.3; 0.91 | 0.2; 0.95 |
| | Group | 19.9; 1.02 × 10 ⁻⁰⁵ | 24.6; 1.04 × 10 ⁻⁰⁶ | 14.4; 0.0002 | 5.9; 0.02 | 8.2; 0.005 |
| | Stimulus | 0.4; 0.6 | 0.2; 0.6 | 0.003; 0.96 | 0.6; 0.4 | 0.3; 0.6 |
| | Window | 5.2; 0.00042 | 8.3; 1.96 × 10 ⁻⁰⁶ | 13.9; 1.12 × 10 ⁻¹⁰ | 9.8; 1.46 × 10 ⁻⁰⁷ | 7.2; 1.24 × 10 ⁻⁰⁵ |
| | Group X Stimulus | 0.7; 0.4 | 0.99; 0.3 | 0.03; 0.9 | 0.04; 0.8 | 0.2; 0.7 |
| | Group X Window | 3.8; 0.0047 | 4.9; 0.0007 | 1.9; 0.1 | 2.2; 0.07 | 0.8; 0.5 |
| | Stimulus X Window | 0.2; 0.9 | 0.3; 0.9 | 0.1; 0.9 | 0.1; 0.9 | 0.7; 0.6 |
| | Group X Stimulus X Window | 0.5; 0.7 | 0.4; 0.8 | 0.2; 0.9 | 0.2; 0.9 | 0.3; 0.9 |

corresponding to the categorization of the stimulus (~ 258 ms). That is to say that this method allowed us to discern in which stage of cognitive processing there was a greater EEG signal energy that might help explain the observed similar behavioral results.

Future work remains to analyze possible cellular mechanisms that lead to increased EEG signal energy for specific bands in one population than in another during a Stroop task. MRI methodologies would be required as it might be possible to have effects of disconnection and/or reorganization of neural networks that could lead to the observed higher energy (Amoroso et al., 2018; Li and Liu, 2019; Long et al., 2019). For instance, using EEG, effects in the cortical connectivity related to memory performance in cognitive decline have been shown (Vecchio et al., 2016), whereas using fMRI it has been shown that disruption of the salience network is related to cognitive decline in elderly people (La Corte et al., 2016; Onoda et al., 2012). Another study found that long-range connections may be more vulnerable to aging effects than short-range connections and that, in addition to the default mode network, the dorsal attention network is also sensitive to aging effects (Tomasi and Volkow, 2012). The methodology presented here, complemented with traditional ERP analysis and another imaging techniques, could shed light in the underlying process and effects of this observed higher energy signal in the Theta-EEG elderly.

4.1. Total energy analysis

The results at the behavioral level showed that there were no major differences between the groups. These results were expected if we consider that the difference between groups were only at the electrophysiological level in the quantitative resting state EEG analysis. Furthermore, the Theta-EEG and Normal-EEG groups showed a Stroop effect (i.e., longer reaction times for Interference stimuli) and they answered with similar efficacy despite the differences in their resting EEG (Table 3).

During the performance of the counting Stroop task we observed that, for both types of stimuli, the Theta-EEG group showed a higher energy in delta, theta, and alpha bands than the Normal-EEG group (Figs. 1 and 2). Given that the total energy is related to the number of synchronized active neurons and that no major differences between groups were observed in the performance of the counting Stroop task, we think that this higher energy reflects neurobiological adaptations taking place in the Theta-EEG group that allow them to cope with the cognitive demands of this task.

In fMRI it has been observed that the healthy elderly presented a greater neural activity during the performance of Stroop tasks than young subjects (Cabeza, 2002; Langenecker et al., 2004; Mathis et al., 2009; Milham et al., 2002; Zysset et al., 2007). We suggest that the increased energy observed in the Theta-EEG group could also be related to greater neuronal activity and that this augmented energy might reflect induced compensatory neurobiological adaptations to achieve an optimum performance (Mathis et al., 2009; Zysset et al., 2007) or it may reflect a difficulty in recruiting specialized neuronal circuits (Cabeza, 2002). Furthermore, in fMRI and ERP studies, the elderly with mild cognitive impairment (MCI) or with electrophysiological risk for cognitive decline exhibited greater brain activity than the healthy elderly (Kaufmann et al., 2008; Sánchez-Moguel et al., 2018). From the point of view of the performance of the task, it is evident that this compensatory mechanism is effective in both the elderly affected by MCI and the Theta-EEG group. However, a higher energy or greater neuronal activity in unspecialized neuronal circuits might trigger anomalous cellular processes that might be hallmarks of neurodegenerative diseases (Mattson and Arumugam, 2018), making this compensatory mechanism ineffective in the long term. The affected elderly will then have an anomalous activation of the involved circuits, and they will show a dysregulated energetic metabolism (Mattson and Arumugam, 2018).

The greater signal energy in the Theta-EEG group observed in delta and theta bands agrees with the finding that increased activity in these

bands predicts the development of cognitive impairment (Prichep et al., 2006; van der Hiele et al., 2008), as shown in Figs. 1, 2, 4, and 9. On the other hand, some studies suggest that increases in alpha power are related to success in inhibiting irrelevant information (Herrmann and Knight, 2001; Werkle-Bergner et al., 2012). This set of works supports our interpretation that the higher alpha energy in the Theta-EEG group is related to a good performance of this group in the task. Furthermore, the greater energy in the alpha band in the Theta-EEG group can be explained by a topographic reorganization of the alpha rhythm during aging in which it is biased towards more frontal regions (Evans and Abarbanel, 1999), as shown in Fig. 7. As mentioned earlier, these EEG changes are exacerbated in patients with dementia or MCI (Prichep et al., 1994; Weisz and Czigler, 2006).

It is hypothesized that the brain is structured and works in a way that minimizes free-energy. This free-energy principle rests on the fact that biological agents such as the brain maintains an homeostatic balance to counteract disorder (Friston, 2010, 2009; Friston et al., 2006). It is possible that the increased energy in the Theta-EEG group is involved in maintaining this homeostatic balance. However, over time the increased energy can promote neural metabolic imbalances more rapidly, causing the development of cognitive impairment. Future work remains to elucidate the mechanisms that lead to this increased EEG signal energy.

4.2. Analysis of relative energy

There was a greater relative energy in both EEG groups in the delta and theta bands compared to the other bands (Fig. 3). For the Theta-EEG group, the relative energy in delta band was greater than for the Normal-EEG group; this relationship reverts in beta and gamma bands (Fig. 3). Patients at risk of cognitive impairment (Prichep et al., 2006; van der Hiele et al., 2008) or who transition from MCI to Alzheimer's disease (Huang et al., 2000; Jelic et al., 2000; Rossini et al., 2006) show an increase in delta and theta power and a decrease in the beta relative power. The beta band is sensitive to the discrimination of Interference and No Interference stimuli in Stroop tasks (Schack et al., 1999), while the gamma band has a prominent role in the coupling of excitatory and inhibitory neuronal networks (Fries, 2009). This lower energy in beta and gamma bands, in addition to the increased theta activity in the Theta-EEG group, agree with the inhibitory control impairment at the electrophysiological level previously reported by Sánchez-Moguel et al. (2018). Based on the reported higher risk of cognitive impairment of the Theta-EEG group (Prichep et al., 2006), we suggest that the greater relative energy in delta band and the lower relative energy in beta and gamma bands during the performance of the Stroop task may be related to the progression to MCI. It would be interesting to study if the observed changes in energy in the above-mentioned frequency bands could be used as a complementary biomarker of risk of cognitive impairment.

4.3. Analysis of total energy across time windows

The greater total energy in both EEG groups occurred in the 258–516 ms window for all bands, as shown in Figs. 4, 5, and 8. In ERP studies, it has been observed that this time window is sensitive to the categorization of interference and no interference words (Zurrón et al., 2009; Sánchez-Moguel et al., 2018). Then, we interpret that this greater energy is related to stimuli categorization. The total energy for this time window was higher for the Theta-EEG group in the theta and alpha bands. Thus, we can hypothesize that the increase in the theta band was because the Theta-EEG population already had excess theta activity in their resting state EEG. We can also relate the increase in alpha band energy in the Theta-EEG group (Fig. 8) to a greater difficulty in inhibitory processing in this group, previously reported by Sánchez-Moguel et al. (2018). We interpret that the combination of increased energy in alpha and theta bands (Fig. 1) reflect neurobiological adaptive mechanisms that allow the Theta-EEG group to discriminate the stimuli with a similar efficiency as the Normal-EEG group.

The total energy for each stimulus condition in the different bands was similar within each EEG group (Figs. 1, 8, and Table 1, Appendix B). This is an interesting result given the increased complexity of the Interference as compared to the No Interference stimuli because reading and counting processes are in competition (Bush et al., 2006; West and Alain, 2000) causing the response times to be longer in Interference stimuli. There was no difference in energy from window to window between stimulus conditions but, considering that for the Interference stimulus the average response time is longer (Table 3), we hypothesize that subjects integrate more energy across time under the Interference stimulus than under the No Interference stimulus. In other words, the variable of interest to better differentiate between stimuli in our experiment could not be directly the energy, but the integral of the energy between the beginning of the task and the response time of the individual. This analysis would be similar to that done when there is a signal $s(t)$ whose period is T and uses the "pulse energy" as a measure, which is defined as the integral of the instantaneous power $s(t)^2$ with respect to the time in a period T of the signal. The hypothesis is that, in elderly adults, the processing of Interference and No Interference stimuli demands similar neuronal resources when comparing the same time windows. Nevertheless, to give a correct answer, patients would need to integrate more energy for the Interference stimuli. This hypothesis should be tested in future research.

Wavelet analysis outperformed STFT when exploring several time windows across low and high frequency bands as delta, theta, alpha and beta bands could be distinguished only with wavelet analysis. Furthermore, by wavelet analysis we revealed that energy increase in delta band in the Theta-EEG group was composed by a slow wave [0, 1.9531] Hz and the "typical" delta band [1.9531–3.9063] Hz (Figs. 4, 8 and 10). Some studies have explored the role of slow waves (<1 Hz) in awake states suggesting that the increase in these waves modulates higher frequency bands such as theta and alpha bands (Kirov et al., 2009; Koo-Poeggel et al., 2019). Studies in elderly at risk of cognitive impairment will be needed to test the role of this slow wave in promoting behavioral deficits.

Recent studies in elderly that also applied wavelet analysis on EEG signals obtained during the performance of cognitive tasks support that theta and alpha frequencies are modulated during ageing. Using a semantic memory task, Alejandro et al. (2021) showed enhanced theta and less decrease of alpha power in older subjects compared to young adults despite that there was no difference in the number of correct responses between groups. The authors suggest that the observed changes may indicate reductions in attentional processing in the older group that might be compensated by higher retrieval efforts to achieve the same behavioral performance. Henry et al. (2017) reported that alpha activity in elderly was suppressed during an auditory gap-detection task while the opposite was observed in young adults; no behavioral differences between groups were reported. The authors hypothesize that alpha suppression reflects that elderly may use a different strategy to allow attention to fluctuate rhythmically.

Our current findings lead us to propose that using wavelets and more than five windows allows a straightforward dissection of signal energy in the EEG bands when analyzing ERPs during a Counting Stroop task in a population of elderly. Summarizing, our results, together with the current literature, support that the wavelet methodology ensures a highly precise analysis of the underlying processes that are taking place within the frequency bands of the EEG signals obtained during cognitive tasks.

5. Conclusions

In summary, the signal energy was higher in the Theta-EEG group during a counting Stroop task. The energy analysis of ERP using wavelets showed that during the Stroop task performance: (1) Theta-EEG group exhibits greater total energy in delta, theta, and alpha bands than Normal-EEG group. (2) Theta-EEG group has a higher relative

energy in delta band but less energy in beta and gamma bands compared to Normal-EEG group. (3) In theta and alpha bands, the energy is greater in the Theta-EEG group, specifically in the time window 258–516 ms related to stimulus categorization processing. (4) Theta-EEG group has higher total energy in 258–516, 516–774, and 774–1032 ms windows in delta band. Thus the current findings emphasize the relevance of a wavelet analysis for diagnosis of neurological disorders, as in recent studies (Alturki et al., 2020; Bhattacharyya and Pachori, 2017; Faust et al., 2015).

We presented a novel methodological design through a wavelet transform that provides an accurate quantification of the EEG energy during a counting Stroop task between a group of elderly subjects with increased theta activity in their resting state EEG and another one with a normal EEG. We propose, as one possible mechanism, that this excessive energy in the Theta-EEG group could imply that more neurons are recruited to perform the task with the same efficiency as the Normal-EEG group. However, we do not know if this increased energy is an effective long-term mechanism since neurons could be recruited from unspecialized regions, and there could be cellular and metabolic imbalances that promote progress to cognitive impairment. Furthermore, since the Theta-EEG group participants have a higher risk of developing cognitive impairment and already show inhibitory control detriment at the electrophysiological level, we suggest that this excessive energy is abnormal.

We can conclude that the obtained results show that the proposed methodology accomplishes high accuracy, which is as good as the best existing state-of-the-art mother wavelet approach found in the literature for EEG signals (Al Ghayab et al., 2019; Blanco et al., 1995, 1996, 1997, 1998; Gross, 2014; Korol et al., 2007; Kovach and Gander, 2016; Lopes-Dos-Santos et al., 2018; Nakhnikian et al., 2016; Navajas et al., 2013; Quian Quiroga et al., 1997; Quiroga et al., 2001; Rosenblatt et al., 2014; Rosso et al., 2001; Rosso et al., 2004; Rosso and Hyslop et al., 2005; Rosso et al., 2005; Schrouff et al., 2016; Schütt et al., 2003; Venkata Phanikrishna and Chinara, 2021; Yordanova et al., 2002; Rosso et al., 2006). Importantly, the current methodology outperforms the Short Time Fourier Transform when exploring EEG signals.

Imaging techniques such as fMRI, diffusion tensor imaging, and magnetic resonance spectroscopy, which evaluate the neural networks involved in the task and metabolic expenditure, would complement our findings (Arco et al., 2018; Dimitriadis et al., 2018; Forouzaneshad et al., 2019; Arco et al., 2018; Long et al., 2019). Additionally, we suggest exploring the signal energy during the performance of tasks related to other cognitive processes that are known to be altered in patients at risk of cognitive impairment.

CRedit authorship contribution statement

Sergio M. Sánchez-Moguel: Conceptualization, Methodology, Investigation, Data curation, Writing – original draft, Writing – review & editing, Supervision. **Roman Baravalle:** Conceptualization, Methodology, Software, Supervision, Formal analysis, Writing – review & editing, Visualization, Data curation. **Sofía González-Salinas:** Formal analysis, Writing – original draft, Visualization, Writing – review & editing. **Oswaldo A. Rosso:** Conceptualization, Methodology, Writing – review & editing, Visualization, Data curation, Software, Supervision. **Thalía Fernández:** Resources, Supervision, Project administration, Funding acquisition, Data curation, Writing – review & editing. **Fernando Montani:** Conceptualization, Methodology, Funding acquisition, Project administration, Supervision, Visualization, Data curation, Software, Writing – review & editing.

Acknowledgments

The authors acknowledge Leonor Casanova, Lourdes Lara, Graciela Alatorre-Cruz, and Teresa Alvarez for administrative support; Juan Silva-Pereyra, Erick Pasaye, Ramón Martínez, Susana Angelica Castro

Chavira, Mauricio González-López, and Héctor Belmont for technical assistance; Marbella Espino, MD, for performing the neurological and psychiatric assessment. The study was supported by PAPIIT-DGAPA, projects IN225414 and IN200817. Sergio M. Sánchez-Moguel received a PhD fellowship from CONACYT (no. 245313). The first draft of the present work started during the summer school LACONEU, 2017; Sergio M. Sánchez-Moguel and Roman Baravalle received Fellowships to attend this event. Fernando Montani thanks funding from PUE 22920170100066CO IFLP-CONICET Argentina, PIP 11220130100327CO (2014/2016) CONICET Argentina (F.M.) and project 80120190100127LP Universidad Nacional de La Plata, Argentina.

Appendix A

In Figs A1, A2, A3, A4 and A5 we show boxplots of the total energy averaged across all electrodes for Theta-EEG group in the Interference condition. We examined the effect of using different mother wavelets in the calculation of the energy, for each temporal window (here we show only five of them, but the results were similar when using ten) and each frequency band. The range of the bands was the same as before except for Delta band which involves also the so-called slow wave activity, that is: Delta [0–3.9063] Hz. There were small differences across the different wavelets, however the results did not differ statistically. The statistical results for the 0–258ms window were the following: Delta: $F(4110) = 0.04$, $p = 0.9966$; Theta: $F(4110) = 0.23$, $p = 0.9229$; Alfa: $F(4110) = 0.13$, $p = 0.9718$; Beta: $F(4110) = 0.03$, $p = 0.9988$; Gamma: $F(4110) = 0.01$, $p = 0.9997$. We reached the same conclusion with the other time windows.

Finally, in Fig. A6 we show the mean STFT energy across temporal windows for the Theta-EEG group in Interference condition for Delta band and electrode CPz. The results using the STFT function implemented in Python and MATLAB yields same results (the two-way ANOVA yielding the results for Program: $F(1220) = 3.7 \times 10^{-30}$, $p = 1$, and for Window: $F(4220) = 9.8 \times 10^{-31}$, $p = 1$). The same results were verified for all electrodes and frequency bands.

Appendix B

See Appendix Table B1 here.

References

- Arco, J.E., González-García, C., Díaz-Gutiérrez, P., Ramírez, J., Ruz, M., 2018. Influence of activation pattern estimates and statistical significance tests in fMRI decoding analysis. *J Neurosci Methods* 308, 248–260. <https://doi.org/10.1016/j.jneumeth.2018.06.017>.
- Al Ghayab, H.R., Li, Y., Siuly, S., Abdulla, S., 2019. A feature extraction technique based on tunable Q-factor wavelet transform for brain signal classification. *J. Neurosci. Methods* 2019 15 (312), 43–52. <https://doi.org/10.1016/j.jneumeth.2018.11.014>.
- Alejandro, R.J., Packard, P.A., Steiger, T.K., Fuentesmilla, L., Bunzeck, N., 2021. Semantic congruence drives long-term memory and similarly affects neural retrieval dynamics in young and older adults. *Front. Aging Neurosci.* 14 (13), 683908 <https://doi.org/10.3389/fnagi.2021.683908>.
- Allen, J., 1977. Short term spectral analysis, synthesis, and modification by discrete Fourier transform. *IEEE Trans. Acoust. Speech Signal Process* 25, 235–238. <https://doi.org/10.1109/TASSP.1977.11629500>.
- Alturki, F.A., AlSharabi, K., Abdurraqueeb, A.M., Aljalal, M., 2020. EEG signal analysis for diagnosing neurological disorders using discrete wavelet transform and intelligent techniques. *Sensors* 20, 2505. <https://doi.org/10.3390/s20092505>.
- Amieva, H., 2004. Evidencing inhibitory deficits in Alzheimer's disease through interference effects and shifting disabilities in the Stroop test. *Arch. Clin. Neuropsychol.* 19, 791–803. <https://doi.org/10.1016/j.acn.2003.09.006>.
- Babor, T.F., Higgins-Biddle, J.C., Saunders, J.B., Monteiro, M.G., 2001. AUDIT: the Alcohol Use Disorders Identification Test: Guidelines For Use in Primary Health Care. World Health Organ.,
- Beck, A.T., Ward, C.H., Mendelson, M., Mock, J., Erbaugh, J., 1961. An inventory for measuring depression. *Arch. Gen. Psychiatry* 4, 561–571. <https://doi.org/10.1001/archpsyc.1961.01710120031004>.
- Bhattacharyya, A., Pachori, R.B., 2017. A multivariate approach for patient-specific EEG seizure detection using empirical wavelet transform. *IEEE Trans. Biomed. Eng.* 64, 2003–2015. <https://doi.org/10.1109/TBME.2017.265025>.
- Blanco, S., Quiroga, R.Q., Rosso, O.A., Kochen, S., 1995. Time-frequency analysis of electroencephalogram series. *Phys. Rev. E Stat. Phys. Plasmas Fluids Relat. Inter. Top.* 51 (3), 2624–2631. <https://doi.org/10.1103/physreve.51.2624>.
- Blanco, S., D'Attellis, C.E., Isaacson, S.I., Rosso, O.A., Sirne, R.O., 1996. Time-frequency analysis of electroencephalogram series. II. Gabor Wavelet. *Transforms Phys. Rev. E Stat. Phys. Plasmas Fluids Relat. Inter. Top.* 54 (6), 6661–6672. <https://doi.org/10.1103/physreve.54.6661>.
- Blanco, S., Kochen, S., Rosso, O.A., Salgado, P., 1997. Applying time-frequency analysis to seizure EEG activity. *IEEE Eng. Med Biol. Mag.* 16 (1), 64–71. <https://doi.org/10.1109/51.566156>.
- Blanco, S., Figliola, A., Quiroga, R.Q., Rosso, O.A., Serrano, E., 1998. Time-frequency analysis of electroencephalogram series. III. Wavelet packets and information cost function. *Phys. Rev. E* 57, 932–940. <https://doi.org/10.1103/PhysRevE.57.932>.
- Bush, G., Whalen, P.J., Shin, L.M., Rauch, S.L., 2006. The counting stroop: a cognitive interference task. *Nat. Protoc.* 1, 230–233. <https://doi.org/10.1038/nprot.2006.35>.
- Baravalle, R., Rosso, O.A., Montani, F., 2018. Discriminating imagined and non-imagined tasks in the motor cortex area: entropy-complexity plane with a wavelet decomposition. *Phys A Stat Mech Appl.* 511, 27–39. <https://doi.org/10.1016/j.physa.2018.07.038>.
- Buzsáki, G., 2006. *Rhythms of the Brain*. Oxford University Press, Oxford; New York.
- Cabeza, R., 2002. Hemispheric asymmetry reduction in older adults: the HAROLD model. *Psychol. Aging* 17, 85–100.
- Cabeza, R., Daselaar, S.M., Dolcos, F., Prince, S.E., Budde, M., Nyberg, L., 2004. Task-independent and task-specific age effects on brain activity during working memory, visual attention and episodic retrieval. *Cereb. Cortex* N. Y. N. 1991 (14), 364–375. <https://doi.org/10.1093/cercor/bhg133>.
- Chang, B.S., Schomer, D.L., Niedermeyer, E., 2011. "Normal EEG and sleep: adults and elderly. In: Niedermeyer's Electroencephalography: Basic Principles, Clinical Applications, and Related Fields. Wolters Kluwer, Lippincott Williams & Wilkins, New York, pp. 183–214.
- Cofman, R.R., Wickerhauser, M.V., 1992. Entropy-based algorithms for best basis selection. *IEEE Trans. Inf. Theory* 38, 713–718. <https://doi.org/10.1109/18.119732>.
- Dimitriadis, S.I., Routley, B., Linden, D.E., Singh, K.D., 2018. Reliability of Static and Dynamic Network Metrics in the Resting-State: A MEG-Beamformed Connectivity Analysis. *Front Neurosci.* 12, 506. <https://doi.org/10.3389/fnins.2018.00506>.
- Daubechies, I., 1992. *Ten Lectures on Wavelets*. SIAM.,
- Diamond, A., 2020. Chapter 19 - Executive functions. In: Gallagher, A., Bulteau, C., Cohen, D., Michaud, J.L. (Eds.), *Handbook of Clinical Neurology*. Elsevier, pp. 225–240. <https://doi.org/10.1016/B978-0-444-64150-2.00020-4>.
- Endicott, J., Nee, J., Harrison, W., Blumenthal, R., 1993. Quality of life enjoyment and satisfaction questionnaire: a new measure. *Psychopharmacol. Bull.* 29, 321–326.
- Evans, J.R., Abarbanel, A., 1999. *Introduction to Quantitative EEG and Neurofeedback*. Elsevier.
- Forouzanmehr, P., Abbaspour, A., Fang, C., Cabrerizo, M., Loewenstein, D., Duara, R., Adjouadi, M., 2019. A survey on applications and analysis methods of functional magnetic resonance imaging for Alzheimer's disease. *J Neurosci Methods* 317, 121–140. <https://doi.org/10.1016/j.jneumeth.2018.12.012>.
- Faust, O., Acharya, U.R., Adeli, H., Adeli, A., 2015. Wavelet-based EEG processing for computer-aided seizure detection and epilepsy diagnosis. *Seizure* 26, 56–64. <https://doi.org/10.1016/j.seizure.2015.01.012>.
- Fries, P., 2009. Neuronal gamma-band synchronization as a fundamental process in cortical computation. *Annu. Rev. Neurosci.* 32, 209–224. <https://doi.org/10.1146/annurev.neuro.051508.135603>.
- Friston, K., 2009. The free-energy principle: a rough guide to the brain? *Trends Cogn. Sci.* 13, 293–301. <https://doi.org/10.1016/j.tics.2009.04.005>.
- Friston, K., 2010. The free-energy principle: a unified brain theory? *Nat. Rev. Neurosci.* 11, 127–138. <https://doi.org/10.1038/nrn2787>.
- Friston, K., Kilner, J., Harrison, L., 2006. A free energy principle for the brain. *J. Physiol. Paris* 100, 70–87. <https://doi.org/10.1016/j.jphysparis.2006.10.001>.
- Goupillaud, P., Grossmann, A., Morlet, J., 1984. Cycle-octave and related transforms in seismic signal analysis. *Geoexplor., Seism. Signal Anal. Discrim. III* 23, 85–102. [https://doi.org/10.1016/0016-7142\(84\)90025-5](https://doi.org/10.1016/0016-7142(84)90025-5).
- Gratton, G., Coles, M.G.H., Donchin, E., 1983. A new method for off-line removal of ocular artifact. *Electroencephalogr. Clin. Neurophysiol.* 55, 468–484. [https://doi.org/10.1016/0013-4694\(83\)90135-9](https://doi.org/10.1016/0013-4694(83)90135-9).
- Gross, J., 2014. Analytical methods and experimental approaches for electrophysiological studies of brain oscillations. *J. Neurosci. Methods* 228 (100), 57–66. <https://doi.org/10.1016/j.jneumeth.2014.03.007>.
- Henry, M.J., Herrmann, B., Künke, D., Obleser, J., 2017. Aging affects the balance of neural entrainment and top-down neural modulation in the listening brain. *Nat. Commun.* 7, 15801. <https://doi.org/10.1038/ncomms15801>.
- Hernández, J.L., Valdés, P., Biscay, R., Virues, T., Szava, S., Bosch, J., Riquenes, A., Clark, I., 1994. A global scale factor in brain topography. *Int. J. Neurosci.* 76, 267–278. <https://doi.org/10.3109/00207459408986009>.
- Herrmann, C.S., Knight, R.T., 2001. Mechanisms of human attention: event-related potentials and oscillations. *Neurosci. Biobehav. Rev.* 25, 465–476. [https://doi.org/10.1016/s0149-7634\(01\)00027-6](https://doi.org/10.1016/s0149-7634(01)00027-6).
- Huang, C., Wahlund, L., Dierks, T., Julin, P., Winblad, B., Jelic, V., 2000. Discrimination of Alzheimer's disease and mild cognitive impairment by equivalent EEG sources: a cross-sectional and longitudinal study. *Clin. Neurophysiol. J. Int. Fed. Clin. Neurophysiol.* 111, 1961–1967.
- Jelic, V., Johansson, S.E., Almkvist, O., Shiget, M., Julin, P., Nordberg, A., Winblad, B., Wahlund, L.O., 2000. Quantitative electroencephalography in mild cognitive impairment: longitudinal changes and possible prediction of Alzheimer's disease. *Neurobiol. Aging* 21, 533–540.

- Kaufmann, L., Ischebeck, A., Weiss, E., Koppelstaetter, F., Siedentopf, C., Vogel, S.E., Gotwald, T., Marksteiner, J., Wood, G., 2008. An fMRI study of the numerical Stroop task in individuals with and without minimal cognitive impairment. *Cortex* 44, 1248–1255. <https://doi.org/10.1016/j.cortex.2007.11.009>.
- Kirov, R., Weiss, C., Siebner, H.R., Born, J., Marshall, L., 2009. Slow oscillation electrical brain stimulation during waking promotes EEG theta activity and memory encoding. *Proc. Natl. Acad. Sci. U. S. A.* 106, 15460–15465. <https://doi.org/10.1073/pnas.0904438106>.
- Koo-Poeggel, P., Böttger, V., Marshall, L., 2019. Distinct montages of slow oscillatory transcranial direct current stimulation (so-tDCS) constitute different mechanisms during quiet wakefulness. *Brain Sci.* 9, 324. <https://doi.org/10.3390/brainsci9110324>.
- Korol, A.M., Rasia, M.J., Rosso, O.A., 2007. Alterations of thalamic erythrocytes detected by wavelet entropy. *Physica A* 375, 257–264. <https://doi.org/10.1016/j.physa.2005.12.074>.
- Kovach, C.K., Gander, P.E., 2016. The demodulated band transform. *J. Neurosci. Methods* 261, 135–154. <https://doi.org/10.1016/j.jneumeth.2015.12.004>.
- La Corte, V., Sperduti, M., Malherbe, C., Vialatte, F., Lion, S., Gallarda, T., Oppenheim, C., Piolino, P., 2016. Cognitive decline and reorganization of functional connectivity in healthy aging: the pivotal role of the salience network in the prediction of Age and cognitive performances. *Front. Aging Neurosci.* 8, 204. <https://doi.org/10.3389/fnagi.2016.00204>.
- Langenecker, S.A., Nielson, K.A., Rao, S.M., 2004. fMRI of healthy older adults during Stroop interference. *NeuroImage* 21, 192–200. <https://doi.org/10.1016/j.neuroimage.2003.08.027>.
- Lopes da Silva, F.H., 2011. Neurocognitive processes and the EEG/MEG. In: Schomer, D. L., Lopes Da Silva, F.H. (Eds.), *Niedermeyer's Electroencephalography: Basic Principles, Clinical Applications, and Related Fields*. Wolters Kluwer, Lippincott Williams & Wilkins, New York, NY, pp. 1083–1112.
- Lopes-dos-Santos, V., Panzeri, S., Kayser, C., Diamond, M.E., Quiñero, R., 2015. Extracting information in spike time patterns with wavelets and information theory. *J. Neurophysiol.* 113, 1015–1033. <https://doi.org/10.1152/jn.00380.2014>.
- Long, Z., Liu, L., Gao, Z., Chen, M., Yao, L., 2018. A semi-blind online dictionary learning approach for fMRI data. *J. Neurosci. Methods* 323, 1–12. <https://doi.org/10.1016/j.jneumeth.2019.03.014>.
- Lopes-Dos-Santos, V., Rey, H.G., Navajas, J., Quiñero, R., 2018. Extracting information from the shape and spatial distribution of evoked potentials. *J. Neurosci. Methods* 15 (296), 12–22. <https://doi.org/10.1016/j.jneumeth.2017.12.01>.
- MacLeod, C.M., 1991. Half a century of research on the Stroop effect: an integrative review. *Psychol. Bull.* 109, 163–203.
- Mallat, S., 2008. *A Wavelet Tour of Signal Processing, third ed.* Academic Press.
- Mathis, A., Schunck, T., Erb, G., Namer, I.J., Luthringer, R., 2009. The effect of aging on the inhibitory function in middle-aged subjects: a functional MRI study coupled with a color-matched Stroop task. *Int. J. Geriatr. Psychiatry* 24, 1062–1071. <https://doi.org/10.1002/gps.2222>.
- Mattson, M.P., Arumugam, T.V., 2018. Hallmarks of brain aging: adaptive and pathological modification by metabolic states. *Cell Metab.* 27, 1176–1199. <https://doi.org/10.1016/j.cmet.2018.05.011>.
- Milham, M.P., Erickson, K.I., Banich, M.T., Kramer, A.F., Webb, A., Wszalek, T., Cohen, N.J., 2002. Attentional control in the aging brain: insights from an fMRI study of the Stroop task. *Brain Cogn.* 49, 277–296. <https://doi.org/10.1006/brcg.2001.1501>.
- Nakhnikian, A., Ito, S., Dwiell, L.L., et al., 2016. A novel cross-frequency coupling detection method using the generalized Morse wavelets. *J. Neurosci. Methods* 269, 61–73. <https://doi.org/10.1016/j.jneumeth.2016.04.019>.
- Navajas, J., Ahmadi, M., Quiñero, R., 2013. Uncovering the mechanisms of conscious face perception: a single-trial study of the N170 responses. *J. Neurosci.* 33, 1337–1343. <https://doi.org/10.1523/JNEUROSCI.1226-12.2013>.
- Nielsen, M., 2001. On the construction and frequency localization of finite orthogonal quadrature filters. *J. Approx. Theory* 108, 36–52. <https://doi.org/10.1006/jath.2000.3514>.
- Nyquist, H., 1928. Certain topics in telegraph transmission theory. *Trans. Am. Inst. Electr. Eng.* 47, 617–644. <https://doi.org/10.1109/T-AIEE.1928.5055024>.
- Onoda, K., Ishihara, M., Yamaguchi, S., 2012. Decreased functional connectivity by aging is associated with cognitive decline. *J. Cogn. Neurosci.* 24, 2186–2198. <https://doi.org/10.1162/jocn.2012.0269>.
- Ortiz-Rosario, A., Adeli, H., Buford, J.A., 2015. Wavelet methodology to improve single unit isolation in primary motor cortex cells. *J. Neurosci. Methods* 246, 106–118. <https://doi.org/10.1016/j.jneumeth.2015.03.014>.
- Ostrosky-Solís, F., Ardila, A., Rosselli, M., 1999. NEUROPSI: A brief neuropsychological test battery in Spanish with norms by age and educational level. *J. Int. Neuropsychol. Soc.* 5, 413–433.
- Percival, D.B., Walden, A.T., 2000. *Wavelet Methods for Time Series Analysis*. Cambridge University Press.
- Prichep, L.S., John, E.R., Ferris, S.H., Reisberg, B., Almas, M., Alper, K., Cancro, R., 1994. Quantitative eeg correlates of cognitive deterioration in the elderly. *Neurobiol. Aging* 15, 85–90.
- Prichep, L.S., John, E.R., Ferris, S.H., Rausch, L., Fang, Z., Cancro, R., Torossian, C., Reisberg, B., 2006. Prediction of longitudinal cognitive decline in normal elderly with subjective complaints using electrophysiological imaging. *Neurobiol. Aging* 27, 471–481. <https://doi.org/10.1016/j.neurobiolaging.2005.07.021>.
- Quiñero, R., Panzeri, S., 2009. Extracting information from neuronal populations: information theory and decoding approaches. *Nat. Rev. Neurosci.* 10, 173–185. doi: 10.1038/nrn2578.
- Quiñero, R., Blanco, S., Rosso, O.A., García, H., Rabinowicz, A., 1997. Searching for hidden information with gabor transform in generalized tonic-clonic seizures. *Electro Clin. Neurophysiol.* 103 (4), 434–439. [https://doi.org/10.1016/s0013-4694\(97\)00031-x](https://doi.org/10.1016/s0013-4694(97)00031-x).
- Quiñero, R.Q., Rosso, O.A., Başar, E., Schürmann, M., 2001. Wavelet entropy in event-related potentials: a new method shows ordering of EEG oscillations. *Biol. Cyber* 84 (4), 291–299. <https://doi.org/10.1007/s004220000212>.
- Ramos-Goicoa, M., Galdo-Álvarez, S., Díaz, F., Zurrón, M., 2016. Effect of normal aging and of mild cognitive impairment on event-related potentials to a stroop color-word task. *J. Alzheimers Dis.* 52, 1487–1501. <https://doi.org/10.3233/JAD-151031>.
- Reisberg, B., Ferris, S.H., de Leon, M.J., Crook, T., 1982. The global deterioration scale for assessment of primary degenerative dementia. *Am. J. Psychiatry* 139, 1136–1139. <https://doi.org/10.1176/ajp.139.9.1136>.
- Reisberg, B., Ferris, S.H., Kluger, A., Franssen, E., Wegiel, J., de Leon, M.J., 2008. Mild cognitive impairment (MCI): a historical perspective. *Int. Psychogeriatr.* 20, 18–31. <https://doi.org/10.1017/S1041610207006394>.
- Rey-Mermet, A., Gade, M., 2018. Inhibition in aging: what is preserved? what declines? a meta-analysis. *Psychon. Bull. Rev.* 25, 1695–1716. <https://doi.org/10.3758/s13423-017-1384-7>.
- Román Lapuente, F., Sánchez Navarro, J.P., 1998. Cambios neuropsicológicos asociados al envejecimiento normal. *Psicol.* 14, 27–43.
- Rosenblatt, M., Figliola, A., Paccosi, G., Serrano, G., Rosso, O.A., 2014. A quantitative analysis of an EEG epileptic records based on multiresolution wavelet coefficients. *Entropy* 16, 5976–6005. <https://doi.org/10.3390/e16115976>.
- Rossini, P.M., Del Percio, C., Pasqualetti, P., Cassetta, E., Binetti, G., Dal Forno, G., Ferreri, F., Frisoni, G., Chioyenda, P., Miniussi, C., Parisi, L., Tombini, M., Vecchio, F., Babiloni, C., 2006. Conversion from mild cognitive impairment to Alzheimer's disease is predicted by sources and coherence of brain electroencephalography rhythms. *Neuroscience* 143, 793–803. <https://doi.org/10.1016/j.neuroscience.2006.08.049>.
- Rosso, O.A., Blanco, S., Yordanova, J., Kolev, V., Figliola, A., Schürmann, M., Başar, E., 2001. Wavelet entropy: a new tool for analysis of short duration brain electrical signals. *J. Neurosci. Methods* 105 (1), 65–75. [https://doi.org/10.1016/s0165-0270\(00\)00356-3](https://doi.org/10.1016/s0165-0270(00)00356-3).
- Rosso, O.A., Figliola, A., Creso, J., Serrano, E., 2004. Analysis of wavelet filtered tonic-clonic electroencephalogram recordings. *Med. Biol. Eng. Comput.* 42, 516–523. <https://doi.org/10.1007/BF02350993>.
- Rosso, O.A., Martin, M.T., Plastino, A., 2005. Evidence of self-organization in brain electrical activity using wavelet-based informational tools. *Phys. A Stat. Mech. It Appl.* 347, 444–464. <https://doi.org/10.1016/j.physa.2004.08.085>.
- Rosso, O.A., Hyslop, W., Gerlach, S., Smith, R.L.L., Rostas, J., Hunter, M., 2005. Quantitative EEG analysis of the maturational changes associated with childhood absence epilepsy. *Phys. A Stat. Mech. It Appl.* 356, 184–189. <https://doi.org/10.1016/j.physa.2005.05.034>.
- Rosso, O.A., Martin, M.T., Plastino, A., 2005. Evidence of self-organization in brain electrical activity using wavelet based informational tools. *Phys. A Stat. Mech. It Appl.* 347, 444–464. <https://doi.org/10.1016/j.physa.2004.08.085>.
- Rosso, O.A., Martin, M.T., Figliola, A., Keller, K., Plastino, A., 2006. EEG analysis using wavelet-based information tools. *J. Neurosci. Methods* 153, 163–182. <https://doi.org/10.1016/j.jneumeth.2005.10.009>.
- Sánchez-Moguel, S.M., Alatorre-Cruz, G.C., Silva-Pereyra, J., González-Salinas, S., Sánchez-Lopez, J., Otero-Ojeda, G.A., Fernández, T., 2018. Two different populations within the healthy elderly: lack of conflict detection in those at risk of cognitive decline. *Front. Hum. Neurosci.* 11. <https://doi.org/10.3389/fnhum.2017.00658>.
- Schack, B., Chen, A.C., Mescha, S., Witte, H., 1999. Instantaneous EEG coherence analysis during the Stroop task. *Clin. Neurophysiol. J. Int. Fed. Clin. Neurophysiol.* 110, 1410–1426.
- Schrouff, J., Mourão-Miranda, J., Phillips, C., Parvizi, J., 2016. Decoding intracranial EEG data with multiple kernel learning method. *J. Neurosci. Methods* 261, 19–28. <https://doi.org/10.1016/j.jneumeth.2015.11.028>.
- Schütt, A., Ito, I., Rosso, O.A., Figliola, A., 2003. Wavelet analysis can sensitively describe dynamics ethanol evoked local field potentials of the slug (*Limax marginatus*) brain. *J. Neurosci. Methods* 129 (2), 135–150. [https://doi.org/10.1016/s0165-0270\(03\)00200-0](https://doi.org/10.1016/s0165-0270(03)00200-0).
- Shannon, C.E., 1949. Communication in the presence of noise. *Proc. IRE* 37, 10–21. <https://doi.org/10.1109/JRPROC.1949.232969>.
- Thomas, A.K., Dave, J.B., Bonura, B.M., 2010. Theoretical perspectives on cognitive aging. In: Armstrong, C.L., Morrow, L. (Eds.), *Handbook of Medical Neuropsychology: Applications of Cognitive Neuroscience*. Springer New York, New York, NY, pp. 297–313. https://doi.org/10.1007/978-1-4419-1364-7_16.
- Tomasi, D., Volkow, N.D., 2012. Aging and functional brain networks. *Mol. Psychiatry* 17 (471), 549–558. <https://doi.org/10.1038/mp.2011.81>.
- Torrence, C., Compo, G.P., 1998. A practical guide to wavelet analysis. *Bull. Am. Meteorol. Soc.* 79, 61–78. [https://doi.org/10.1175/1520-0477\(1998\)079<0061:APGTWA>2.0.CO;2](https://doi.org/10.1175/1520-0477(1998)079<0061:APGTWA>2.0.CO;2).
- Valdés, P., Biscay, R., Galán, L., Bosch, J., Zsava, S., Virués, T., 1990. High resolution spectral EEG norms topography. *Brain Topogr.* 3, 281–282.
- van der Hiele, K., Bollen, E.L., Vein, A.A., Reijntjes, R.H., Westendorp, R.G., van Buchem, M.A., Middelkoop, H.A., van Dijk, J.G., 2008. EEG markers of future cognitive performance in the elderly. *J. Clin. Neurophysiol.* 25, 83–89.
- Vecchio, F., Miraglia, F., Quaranta, D., Granata, G., Romanello, R., Marra, C., Bramanti, P., Rossini, P.M., 2016. Cortical connectivity and memory performance in cognitive decline: a study via graph theory from EEG data. *Neuroscience* 316, 143–150. <https://doi.org/10.1016/j.neuroscience.2015.12.036>.
- Venkata Phanikrishna, B., Chinara, S., 2021. Automatic classification methods for detecting drowsiness using wavelet packet transform extracted time-domain features

- from single-channel EEG signal. *J. Neurosci. Methods* 347, 108927. <https://doi.org/10.1016/j.jneumeth.2020.108927>.
- Wechsler, D., 2003. *Wais-III Escala Wechsler de Inteligencia Para Adultos-III*, second ed. Manual Moderno, México.
- Weisz, J., Czigler, I., 2006. Age and novelty: event-related brain potentials and autonomic activity. *Psychophysiology* 43, 261–271. <https://doi.org/10.1111/j.1469-8986.2006.00395.x>.
- Werkle-Bergner, M., Freunberger, R., Sander, M.C., Lindenberger, U., Klimesch, W., 2012. Inter-individual performance differences in younger and older adults differentially relate to amplitude modulations and phase stability of oscillations controlling working memory contents. *NeuroImage* 60, 71–82. <https://doi.org/10.1016/j.neuroimage.2011.11.071>.
- West, R., Alain, C., 2000. Age-related decline in inhibitory control contributes to the increased stroop effect observed in older adults. *Psychophysiology* 37, 179–189.
- Yesavage, J.A., Brink, T.L., Rose, T.L., Lum, O., Huang, V., Adey, M., Leirer, V.O., 1982. Development and validation of a geriatric depression screening scale: a preliminary report. *J. Psychiatr. Res.* 17, 37–49.
- Yordanova, J., Kolev, V., Rosso, O.A., Schürmann, M., Sakowitz, O.W., Ozgören, M., Basar, E., 2002. Wavelet entropy analysis of event-related potentials indicates modality-independent theta dominance. *J. Neurosci. Methods* 117 (1), 99–109. [https://doi.org/10.1016/S0165-0270\(02\)00095-x](https://doi.org/10.1016/S0165-0270(02)00095-x).
- Zurrón, M., Pouso, M., Lindín, M., Galdo, S., Díaz, F., 2009. Event-related potentials with the stroop colour-word task: timing of semantic conflict. *Int. J. Psychophysiol.* 72, 246–252. <https://doi.org/10.1016/j.ijpsycho.2009.01.002>.
- Zysset, S., Schroeter, M.L., Neumann, J., Yves von Cramon, D., 2007. Stroop interference, hemodynamic response and aging: an event-related fMRI study. *Neurobiol. Aging* 28, 937–946. <https://doi.org/10.1016/j.neurobiolaging.2006.05.008>.